The number of strong social bonds is linked to survival in a cooperative bird

Gabriel Munar-Delgado[1,2,*], Matthieu Paquet[3], Babette Fourie[1,2], Franck Theron[1,2], André Ferreira[4], Claire Doutrelant[5,6], Rita Covas[1,2,6]

[1] CIBIO, Centro de Investigação em Biodiversidade e Recursos Genéticos, Universidade do Porto, Vairão, Portugal

[2]BIOPOLIS, Program in genomics, Biodiversity and Land Planning, Vairão, Portugal

[3]SETE, Station d'Écologie Théorique et Expérimentale, CNRS, Moulis, France

[4]Department of Evolutionary Biology and Environmental Studies, University of Zurich, Zurich, Switzerland

[5]CEFE, CNRS, University of Montpellier, EPHE, IRD, Montpellier, France

[6]FitzPatrick Institute of African Ornithology, DST-NRF Centre of Excellence, University of Cape Town, Rondebosch, South Africa

Corresponding author:

Gabriel Munar-Delgado

CIBIO, Rua Padre Armando Quintas nº 7, 4485-661 Vairão

gabriel.munar@gmail.com

ABSTRACT

Recent evidence, particularly from mammals, shows that variation in the quality of social relationships is associated with survival. In parallel, studies across diverse taxa have reported that social network traits can show consistent individual differences over time. However, few studies have assessed whether the specific social traits that predict survival are also repeatable within individuals, limiting our understanding of their contribution to fitness variation. To address this, we used a long-term study of sociable weavers (*Philetairus socius*), a cooperative bird, to quantify individual sociality as the relative number of strong social bonds within colony-year foraging networks, capturing preferential associations. We then estimated its repeatability and association with seasonal survival using multi-state capture–recapture models that account for state-dependent detection. Individual sociality was moderately repeatable across years, indicating consistent differences among individuals despite temporal variation in social environments. Sociality was also positively associated with survival: more social individuals had higher survival probabilities than less social individuals in both winter and summer periods. These findings suggest that sociality may contribute to fitness variation and be subject to selection in this system, adding to the growing evidence that the quality of social bonds has adaptive value across taxa.

Key words: fitness, multi-state capture-recapture, repeatability, social bonds, social network, sociality, survival

INTRODUCTION

Group living is widespread across taxa and provides well-established fitness benefits, including improved access to resources and reduced predation risk (J. Krause et al., 2002).

While early work focused primarily on the costs and benefits of group size (Bilde et al., 2007; Koenig, 1981), more recent studies highlight that individual variation in social relationships within groups (i.e. individual sociality) also plays a key role in fitness outcomes (e.g., Formica et al., 2012; Silk et al., 2010). In particular, a growing body of evidence, largely from mammals, shows that individual sociality can influence survival (reviewed in Snyder-Mackler et al., 2020).

This relationship is thought to arise through multiple, non-mutually exclusive mechanisms across taxa. Higher individual sociality can improve access to resources by reducing vigilance and increasing access to social information about resource availability (De Moor & Brent, 2025). More social individuals have been shown to be better able to locate and exploit novel foraging patches (Aplin et al., 2012) and to exhibit higher survival rates during food-scarce years (Ellis et al., 2017). Social relationships can additionally reduce conspecific harassment and conflict (Cameron et al., 2009). Finally, they may provide direct benefits under challenging environmental conditions, for instance through social thermoregulation, helping individuals cope with both cold (Campbell et al., 2018) and heat stress (Testard et al., 2024).

In this context, whether individual sociality that is linked to survival can be shaped by selection depends on the extent to which it is temporally consistent. The degree to which individual sociality is stable over time may influence whether differences among individuals are persistently exposed to selection (Boake, 1989). While some studies have reported consistent individual differences in social network traits such as degree or strength (Aplin et al., 2015; Blumstein et al., 2013), others have found lower consistency or variation across metrics (e.g., Evans et al., 2021; Plaza et al., 2020). Yet, few studies have jointly assessed the temporal stability of social traits and their relationship with fitness within the same system (but see Vander Wal et al., 2015).

In this study, we assessed whether individual sociality is consistent over time and whether it is associated with survival in the sociable weaver (*Philetairus socius*), a highly cooperative and colonial passerine. Sociable weavers live in relatively stable colonies centred around communal nests, which are built cooperatively, often on camelthorn trees (*Vachellia erioloba*), and contain multiple independent chambers used year-round for roosting and breeding (Maclean, 1973). They are cooperative breeders, with helpers-at-the-nest (usually offspring from previous broods, but also unrelated individuals) assisting in chick provisioning (Covas et al., 2006). Within these colonies, individuals preferentially associate with specific partners. Sociable weavers typically roost in groups inside individual nest chambers, and these roosting associations show temporal stability and non-random structure within colonies (Pacheco, 2022; Paquet et al., 2016). In addition, social associations between breeders and helpers persist across the year, extending beyond the breeding season into foraging contexts (Ferreira et al., 2024), indicating that preferential social bonds can extend across both time and ecological contexts.

Because sociable weavers live and forage in highly cohesive flocks that include most colony members (Lloyd et al., 2018), extracting meaningful social network metrics that reflect individual sociality can be challenging. Networks based on simple co-occurrence at RFID feeders tend to be dense and provide limited information on individual differences, largely capturing overall gregariousness rather than preferential social relationships (Ferreira et al., 2020). We therefore quantified individual sociality based on time-overlapping foraging associations, which better capture social relationships among individuals in this species (Ferreira et al., 2020), and focused on the relative number of strong social bonds to identify preferential and more stable associations that go beyond the general pattern of associations among colony members.

Based on previous results from other systems (Cameron et al., 2009; Ellis et al., 2019; Silk et al., 2010; Thompson & Cords, 2018; reviewed Snyder-Mackler et al., 2020), these closer, stronger, and potentially stable associations within colonies are expected to influence individual survival. In sociable weavers, individuals with a greater number of strong social bonds could benefit from improved access to food resources, as social relationships can shape foraging decisions and access to shared foraging opportunities (Firth et al., 2016; Marshall et al., 2015). In addition, sociable weavers experience frequent agonistic interactions with conspecifics, particularly in the context of access to shared food resources (Rat, 2015). Individuals with more strong social bonds may therefore experience fewer antagonistic interactions, potentially reducing social stress and energetic costs. These individuals may also have increased access to larger roosting groups, which increase nest chamber temperatures and reduce exposure to extreme cold, particularly during winter nights (Paquet et al., 2016). Finally, if strong social bonds partly reflect relationships with helpers at the nest, they may also benefit from the survival advantages associated with receiving help (Paquet et al., 2015).

Given these potential mechanisms, we first investigated whether individual sociality shows temporal consistency across years. We then examined the association between individual sociality and survival using multi-state capture–recapture analysis, predicting that individuals with higher sociality—quantified as the relative number of strong social bonds—would have higher survival probabilities across seasons.

MATERIALS AND METHODS

Site and study species

We studied a population of sociable weavers at Benfontein Nature Reserve in South Africa (28°52′S, 24°50′E). This population has been the focus of a long-term research program initiated in 1993. Since 2008, the population has been regularly monitored through annual captures (see below), and since 2010, breeding has been consistently monitored, with all nestlings that reached nine days of age being ringed and having blood samples taken for sexing and genotyping.

Since 2017, all birds (adults and fledglings) at five colonies have also been marked with a passive integrated transponder (PIT-tag) enclosed in a plastic leg ring (3.3mm; Eccel Technology) to allow detection at RFID feeders (see below). In 2021, a fire destroyed two of those colonies, but in 2022, an additional colony was PIT-tagged, bringing the total number of marked colonies to four.

Mist-nest captures

Resident and recently migrated birds from PIT-tagged colonies are captured annually in September (i.e., at the end of the Southern Hemisphere winter). This was done by placing mist nets around the colony's nest structure before dawn (when the birds were roosting inside the nests) and later flushing them into the nets. Individuals not born in the study population were fitted with a metal ring, PIT-tagged, and had a blood sample taken for sexing (see Supplementary Material for details on age and sex determination). All individuals were released at the site of capture. For this study we used data from 2018 to 2023 (except for 2020 due to COVID-19 restrictions)

RFID data collection and social network metrics

From 2018 to 2023 (except for 2020), we collected association data in a foraging context using RFID-based feeding stations located 80–205 m away from each colony (described in Ferreira et al., 2020). In short, feeding stations consisted of four feeding boxes, each

147 equipped with four small standard plastic bird feeders and four perches fitted with an
148 RFID antenna (Priority1rfid, Melbourne, Australia) connected to a data logger which
149 recorded the birds' visits. Each perch and feeder was designed to only allow one bird to
150 feed at a time. Data were collected from April to June, with data collection conducted
151 usually every three days. This period was chosen to coincide with the end of breeding and
152 the first winter months (which is the dry season, when resources are expected to drop and
153 temperatures fall to below zero, making communal roosting more important; Paquet et
154 al., 2016).

155 For each specific season, we inferred social networks based on the time overlap between
156 individuals at the feeders. Following Ferreira et al. (2020), the strength of the association
157 between two individuals was calculated as the time those two birds spent feeding
158 simultaneously (i.e. exact temporal overlap) in the same feeding box, divided by the sum
159 of the times each individual was present at any of the RFID feeders (i.e. a time-based
160 formulation of the simple ratio index; Ginsberg & Young, 1992). Simultaneous feeding
161 events shorter than 5 seconds were excluded as they reflect displacements instead of
162 associations. This method has been shown to capture the fine-scale social structure within
163 a colony of sociable weavers better than other more commonly used approaches in birds
164 such as co-occurrences (Ferreira et al., 2020). This is because sociable weavers are
165 colonial and tend to forage in cohesive flocks, usually co-occurring at the RFID feeders
166 with most members of their colony.

167 To determine strong social bonds (Gero et al., 2005; Kern & Radford, 2021), we grouped
168 individuals from the same colony and classified the edges between them as either strong
169 or non-strong bonds (Figure 1). For each colony and year, we ranked the edges in
170 descending order based on their association weight. Edges with weight values greater than
171 or equal to the 80th percentile were classified as strong bonds, while the remaining edges

were classified as non-strong bonds (Fourie et al. unpublished results; Camerlenghi et al., 2022). Defining strong bonds using a percentile threshold identifies the strongest associations within each colony-year network and avoids relying on a fixed absolute cut-off that may not be comparable across networks. To assess the robustness of our results to the choice of this threshold, we conducted a sensitivity analysis in which strong bonds were alternatively defined using the 70th and 90th percentiles of edge weights. The subsequent steps of the analysis were repeated using these alternative thresholds.

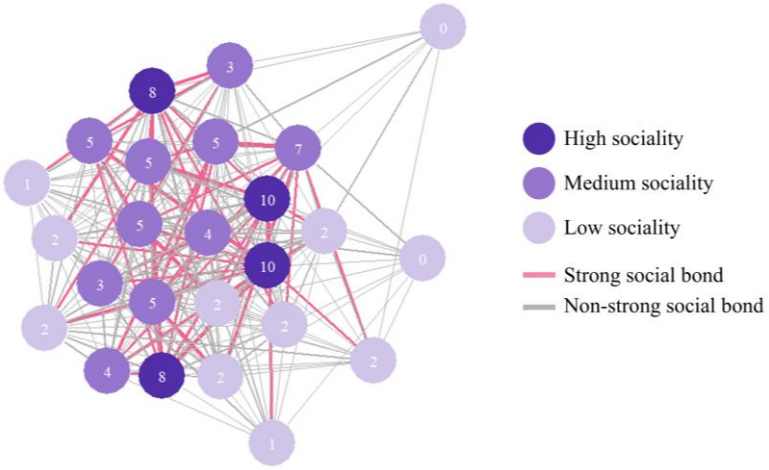

Figure 1. Example social network topology derived from RFID data (Colony 20 in 2021; n = 25 individuals). Nodes represent individuals and edges represent pairwise association strength based on temporal overlap at feeders; edge width is proportional to association strength. Pink edges indicate strong social bonds (edges with weight values ≥ the 80th percentile within this colony-year). The number shown inside each node indicates the number of strong social bonds of that individual. Node colour indicates the individual's sociality category (low, medium, high), defined from the colony-year–

specific distribution of strong bond counts using the 33rd and 66th percentiles. Node positions are determined using a force-directed layout and are shown for visualisation only. Even when inferred from time-overlap data, foraging networks in sociable weavers are typically dense; therefore, meaningful variation is captured primarily by differences in association strength, from which strong social bonds and individual sociality are derived.

Based on this identification of strong bonds, we calculated for each individual the number of such bonds. We then classified individuals into three social status categories based on this number: low, medium, and high. For each year and colony, we determined the 33rd and 66th percentiles of the number of strong bonds each individual had. Individuals with strong bond counts above the 66th percentile were classified as having a high number of social bonds, those between the 33rd and 66th percentiles as having a medium number, and those below the 33rd percentile as having a low number of social bonds. Therefore, the classification depends on the colony-year distribution of strong bonds, which may vary with colony size and social structure. This classification served as the social network metric for our analyses (see Supplementary Material, Table S4, for colony-year–specific colony sizes and category ranges).

This discrete classification of sociality (low, medium, high) enabled the use of a multi-state capture–recapture model (J. D. Lebreton & Cefe, 2002; Schaub et al., 2004). This model allowed us to estimate the transition probabilities from one social status to another from one year to the next, along with specific-state survival probabilities. Additionally, this model also enabled the inclusion of individuals with missing social status data, as long as data had been recorded in at least one year.

Multi-state capture–recapture models

We estimated social status-specific survival, transitions, and detection probabilities of RFID-tagged sociable weavers using a Bayesian multi-state capture-recapture model. Each year (t), we conducted two capture/detection events: one using RFID-feeders (see above) and another with mist nets (see above). Data from RFID-feeders allowed us to estimate individual sociality states (low, medium, high) and provided an additional detection event, while mist-net captures ensured higher and more consistent detection across individuals.

This setup enabled us to estimate survival probabilities based on social status during the intervals between these two events. On the one hand, we estimated the survival probability between the RFID-feeder data collection and the mist net captures within the same year, specifically from July to August (Figure 2). This period largely corresponds to the winter season; therefore, for simplicity, during the analysis, specifications, and results we refer to this estimate as the winter survival probability. On the other hand, we estimated the survival probability between the mist net captures and the RFID-feeder data collection of the following year ($t+1$), specifically from October to April (Figure 2). This period largely corresponds to the spring and summer seasons. For simplicity, and in contrast to the winter survival probability, during the analysis specifications and results we refer to this estimate as the summer survival probability.

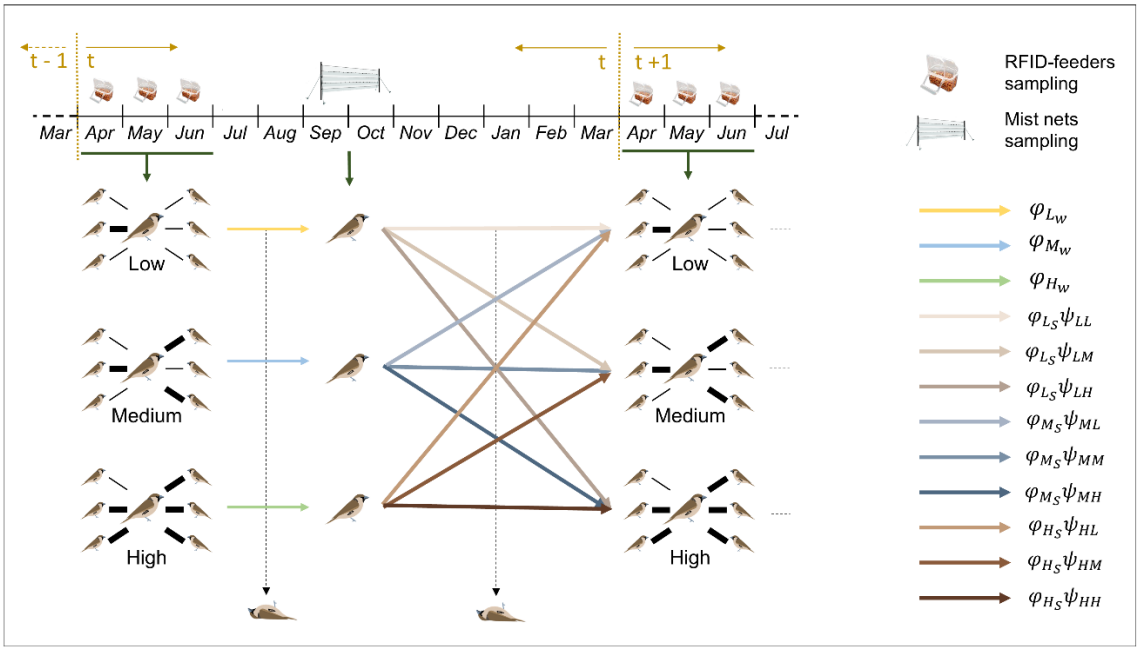

Figure 2. Schematic overview of yearly data collection and the multi-state capture-recapture model. Each yearly time period (t) begins in April with RFID data collection conducted from April to June and ends in March before the next year's RFID-data collection period. During the RFID data collection period, individuals' social status is estimated based on the number of strong social bonds that they have: low (L), medium (M) or high (H). Mist-net captures were conducted in September, at the end of the Southern Hemisphere winter. Between these two periods, individuals can either survive or not, and between consecutive RFID data collection periods, individuals can either remain in the same social status or transition to a different one, provided they survive. The capture-recapture model estimates two survival probabilities: (1) *winter* survival probability, from the RFID data collection period to the mist-net captures within the same year, for low, medium, and highly social individuals, and (2) *summer* survival probability of low, medium, and highly social individuals, conditional on their transition probabilities between social statuses, from the mist-net captures to the RFID data collection period. φ_{X_w} is the winter survival probability of an individual in state X; φ_{X_s} is the summer

survival probability off an individual in state X and ψ_{XY} is the transition probability from state X to state Y from *t* to *t+1*.

With the same model, we also estimated the detection probability conditional on sociable weavers' social status (estimated from RFID-feeder data) at both the RFID feeder and mist-net captures, and the social-status transition probability from one year to the next. Multi-state capture–recapture models explicitly account for state-dependent differences in detection probabilities (Lebreton et al., 2009). This adjustment prevents the underestimation of survival probabilities in groups of individuals that are less likely to be detected due to their state (e.g., low-sociality birds may visit the RFID feeders infrequently; if their lower detection probability isn't modelled, an undetected bird could be wrongly assumed dead). In our study, this approach enabled us to assess the detection probabilities of birds with different sociality levels at both mist-nets and RFID feeders, allowing the model to adjust survival and transition-probability estimates accordingly.

These different survival, transition, and detection probabilities can be represented in the corresponding survival, transition, and detection probability matrices. In the survival and detection matrices, we can represent the different detection probabilities linking the state of an individual (in rows) to the possible observations (in columns) at each data collection occasion within an observation matrix (Θ). In the transition matrices, each row corresponds to the departure state, and each column corresponds to the arrival state of an individual. To improve clarity, we explicitly label the rows and columns of each matrix using the four possible states: L (low sociality), M (medium sociality), H (high sociality), and D (dead). Thus, in all matrices, the rows correspond to the individual's state at time *t*, and the columns represent either the observed state or the state at time *t+1*. In this way, for detection probabilities at the mist-net captures and winter survival probabilities, the matrices were:

276

$$\Theta_n = \begin{array}{c} \begin{matrix} \mathrm{L}_{t+1} & \mathrm{M}_{t+1} & \mathrm{H}_{t+1} & \mathrm{D}_{t+1} \end{matrix} \\ \begin{pmatrix} p_{L_n} & 0 & 0 & 1-p_{L_n} \\ 0 & p_{M_n} & 0 & 1-p_{M_n} \\ 0 & 0 & p_{H_n} & 1-p_{H_n} \\ 0 & 0 & 0 & 1 \end{pmatrix} \end{array} \begin{matrix} \mathrm{L}_t \\ \mathrm{M}_t \\ \mathrm{H}_t \\ \mathrm{D}_t \end{matrix} \qquad \Omega_w = \begin{array}{c} \begin{matrix} \mathrm{L}_{t+1} & \mathrm{M}_{t+1} & \mathrm{H}_{t+1} & \mathrm{D}_{t+1} \end{matrix} \\ \begin{pmatrix} \varphi_{L_w} & 0 & 0 & 1-\varphi_{L_w} \\ 0 & \varphi_{M_w} & 0 & 1-\varphi_{M_w} \\ 0 & 0 & \varphi_{H_w} & 1-\varphi_{H_w} \\ 0 & 0 & 0 & 1 \end{pmatrix} \end{array} \begin{matrix} \mathrm{L}_t \\ \mathrm{M}_t \\ \mathrm{H}_t \\ \mathrm{D}_t \end{matrix}$$

277

278

279 where θ_n is the observation matrix for mist-nets matrix and p_{X_n} is the detection
280 probability at nets of an individual in state X. Ω_w is the winter survival matrix and φ_{X_w}
281 is the winter survival probability off an individual in state X.

282

283 On the other hand, the detection probability matrix at feeders and transition-summer
284 survival matrix were:

$$\Theta_f = \begin{array}{c} \begin{matrix} \mathrm{L}_{t+1} & \mathrm{M}_{t+1} & \mathrm{H}_{t+1} & \mathrm{D}_{t+1} \end{matrix} \\ \begin{pmatrix} p_{L_f} & 0 & 0 & 1-p_{L_f} \\ 0 & p_{M_f} & 0 & 1-p_{M_f} \\ 0 & 0 & p_{H_f} & 1-p_{H_f} \\ 0 & 0 & 0 & 1 \end{pmatrix} \end{array} \begin{matrix} \mathrm{L}_t \\ \mathrm{M}_t \\ \mathrm{H}_t \\ \mathrm{D}_t \end{matrix} \qquad \Omega_s = \begin{array}{c} \begin{matrix} \mathrm{L}_{t+1} & \mathrm{M}_{t+1} & \mathrm{H}_{t+1} & \mathrm{D}_{t+1} \end{matrix} \\ \begin{pmatrix} \varphi_{L_s}\psi_{LL} & \varphi_{L_s}\psi_{LM} & \varphi_{L_s}\psi_{LH} & 1-\varphi_{L_s} \\ \varphi_{M_s}\psi_{ML} & \varphi_{M_s}\psi_{MM} & \varphi_{M_s}\psi_{MH} & 1-\varphi_{M_s} \\ \varphi_{H_s}\psi_{HL} & \varphi_{H_s}\psi_{HM} & \varphi_{H_s}\psi_{HH} & 1-\varphi_{H_s} \\ 0 & 0 & 0 & 1 \end{pmatrix} \end{array} \begin{matrix} \mathrm{L}_t \\ \mathrm{M}_t \\ \mathrm{H}_t \\ \mathrm{D}_t \end{matrix}$$

285

286 where θ_f is the observation matrix for RFID-feeders and p_{X_f} is the recapture probability
287 at RFID-feeders of an individual in state X. Ω_s is the summer survival-transition matrix,
288 φ_{X_s} is the summer survival probability of an individual in state X and ψ_{XY} is the transition
289 probability from state X to state Y from *t* to *t+1*.

290 Detection probabilities for year 2020 ($t = 3$) were set to zero both for the mist-nets and
291 RFID-feeders due to the lack of data collection for that year.

292 **Model fitting**

293 We used NIMBLE (version 1.1.0 of the *nimble* package; De Valpine et al., 2017;
294 NIMBLE Development Team, 2025) to implement our multistate capture-recapture

295 models in a Bayesian framework in Program R, version 4.0.2 (R Core Team, 2020). For
296 all models, a logit link was used. We estimated parameters using vague priors (Table S2).
297 Posterior samples from three independent Markov Chain Monte Carlo (MCMC) chains
298 were based on 70000 iterations with a burn-in period of 35000 iterations and a thinning
299 interval of 20, leading to 5250 posterior MCMC samples. We assessed model
300 convergence both visually and by using the $\hat{R}$ Gelman–Rubin statistic (Gelman & Rubin,
301 1992). Finally, we also performed posterior predictive checks. Mean differences between
302 the state specific survival, transition, and detection probabilities (and their 95% credible
303 intervals) were calculated from the posterior estimates. We considered differences
304 statistically significant when their 95% credible intervals did not overlap zero.

305

306

307 **Covariates and random effects**

308 Our multistate model incorporated several individual covariates (see Supplementary
309 Material for a detailed description) to account for their effects on social survival
310 probabilities in both winter and summer, as well as on transition probabilities and
311 detection probabilities at RFID-feeders. In contrast, we assumed that detection probability
312 at mist nets was independent of covariates because of the mist-net capture method (see
313 above).

314 For survival probabilities in winter and transition/survival probabilities in summer, we
315 included individual age and sex as covariates, with year and the individual's colony as
316 random effects. Age was included because we hypothesized that it could influence
317 survival (Martin, 1995). Sex was included because we hypothesized that survival may
318 differ between males and females (Payevsky, 2021). Individuals for which sex could not

be genetically determined. The individuals' colony and year were included to account for potential inter-colony and annual variation in survival. We allowed age and sex to have different effects on winter and summer survival, as these effects could vary between the two periods. Year and colony random effects were also allowed to differ between winter and summer. Age was centred by subtracting the mean of all observed ages across individuals and years. Sex was centred by subtracting the overall proportion of males across all individuals included in the model. This approach improves the efficiency of MCMC sampling and allowed us to interpret the model intercepts as the social status-specific survival probabilities of an individual with average age and sex ratio in the population (Table S3).

Finally, for the detection probability at RFID-feeders, we included the presence or absence of RFID-feeders at the individual's colony as a covariate since PIT-tagged individuals can migrate to colonies without RFID-feeders but are expected to be less likely detected if no feeders are present at their colony.

See Tables S1-S3 for the detailed models' description.

Repeatability of sociality

To formally assess temporal consistency in individual sociality, we estimated individual repeatability using a Bayesian cumulative threshold model implemented in the R package brms (Bürkner, 2017). Sociality level (low, medium, high) was modelled as an ordered categorical response with a cumulative logit link. Individual identity and colony were included as random intercepts, while age and sex were included as fixed effects. Repeatability was quantified on the latent scale, where the distribution-specific residual variance is fixed to $\pi^2/3$ for the logit link (Nakagawa & Schielzeth, 2013). We estimated

343 model parameters using vague priors. Posterior samples from four independent MCMC
344 chains were based on 4,000 iterations per chain, with a burn-in period of 2,000 iterations,
345 resulting in 8,000 posterior MCMC samples. We assessed model convergence both
346 visually and by using the $\hat{R}$ Gelman–Rubin statistic (Gelman & Rubin, 1992). Posterior
347 distributions and 95% CI were calculated from the posterior samples.

348

349 **RESULTS**

350 **Data and model overview**

351 We captured 661 individuals with mist nets over the study period. Based on RFID-
352 feeders' detections, 430 individuals with known sex were included in the multi-state
353 capture-recapture model, as they had RFID-feeder-based social status data for at least one
354 year (excluding those with data only from the last year, since recapture data was not
355 available for these individuals). Our RFID-feeder social status observation matrix
356 consisted of 702 observations, with 36% corresponding to low, 33% to medium, and 31%
357 to high sociality individuals. Figure S1 provides a descriptive overview of the distribution
358 of observations across age classes, sexes, and sociality categories, together with sample
359 sizes.

360 Overall model diagnostics indicated satisfactory performance of the multi-state capture–
361 recapture model (Figures S2 and S3).

362

363

364 **Repeatability of sociality**

Sociality level showed consistent individual differences across years, with a repeatability of R = 0.32 [95 % CrI: 0.18, 0.47] on the latent scale. In addition, sociality increased slightly with age (0.11 [0.02, 0.20]) and present lower values in females than in males (-1.55 [-2.01, -1.11]) (Table S7).

Detection probabilities

We observed similar detection probabilities based on mist-net captures among individuals with low, medium, and high sociality (0.86 [0.77, 0.93], 0.88 [0.82, 0.94], and 0.88 [0.81, 0.93], respectively; Figure 3; Tables S5 and S6).

Similarly, at the RFID feeders we found no evidence of significant differences in detection probabilities among low-, medium-, and high-sociality individuals (0.48 [0.12, 0.93], 0.32 [0.06, 0.76], and 0.31 [0.07, 0.74], respectively; Figure 3; Tables S5 and S6), although estimates show broad credible intervals, reflecting substantial uncertainty.

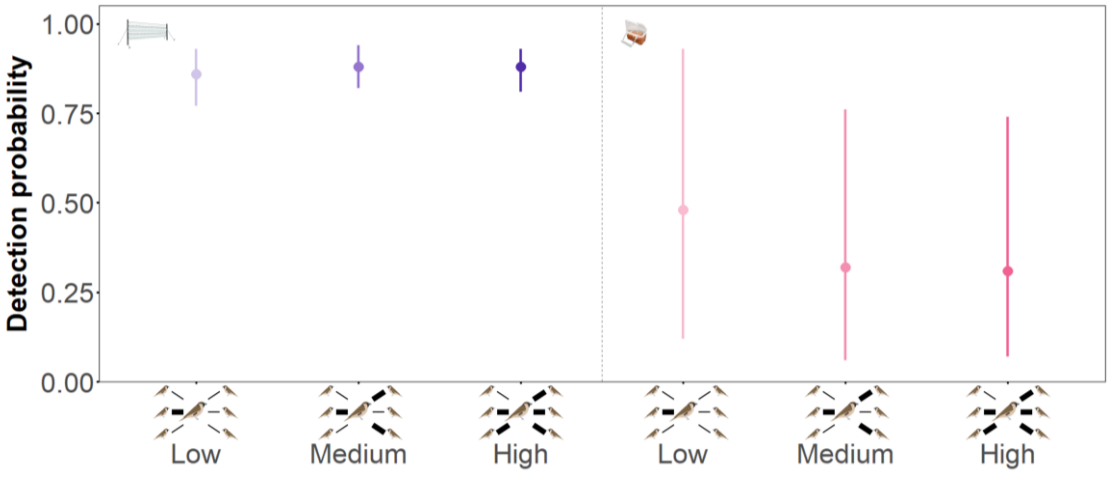

Figure 3. Detection probabilities. Model estimates of detection probabilities for low, medium and high sociality individuals at RFID-feeders (left) and mist-nets (right). Dots represent the posterior mean estimates and bars their 95% credible intervals

Transition probabilities

We found that low-sociality individuals were significantly more likely to remain in the low category (0.47 [0.35, 0.59]) than to shift directly to the high category (0.19 [0.10, 0.30]; Tables S5 and S6). The probability of transitioning from low to medium (0.34 [0.23, 0.47]) fell between those two values, and the differences between remaining low versus transitioning to medium and transitioning to medium versus transitioning to high did not reach statistical significance (Figure 4).

For medium-sociality individuals, we found that they were statistically significantly more likely to remain at the medium level (0.47 [0.35, 0.58]) than to transition to either the low level (0.26 [0.17, 0.36]) or the high level (0.27 [0.19, 0.37]; Tabled S5 and S6). However, there was no statistically significant difference between the likelihoods of transitioning to the low versus the high level (Figure 4).

Finally, for high-sociality individuals, we found that they were statistically significantly more likely to remain at the high level (0 .60 [0.49, 0.70]) than to transition to either the low level (0 .09 [0.04, 0.15]) or the medium level (0 .31 [0.22, 0.43]; Tables S5 and S6). Notably, they were also statistically significantly less likely to transition to the low than to the medium level, again highlighting that abrupt changes in sociality were less common (Figure 4).

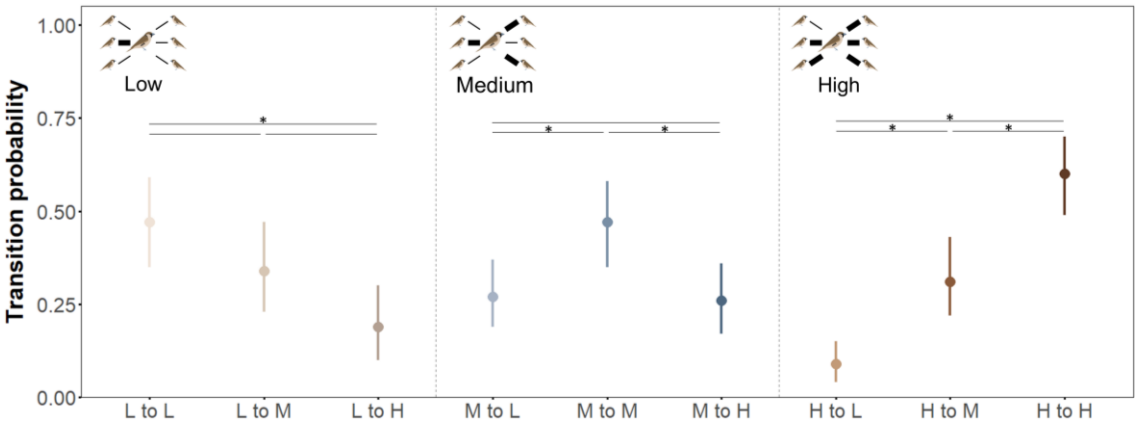

Figure 4. Transition probabilities. Model estimates of transition probabilities for low (L), medium (M), and high (H) social individuals. Dots represent the posterior mean estimates and bars their 95% credible intervals. Asterisks indicate statistically significant differences between transition probabilities.

Survival probabilities

We found that, during the winter period, high-sociality individuals had significantly higher survival probabilities (0.90 [0.79, 0.96]) than low-sociality individuals (0.78 [0.62, 0.89]; Figure 5, Tables S5 and S6), with a posterior median difference of 0.12 (95% CrI: 0.02, 0.25), corresponding to a 12 percentage-point difference in survival probability. Although medium-sociality individuals showed intermediate survival (0.85 [0.72, 0.93]), the difference between medium and low sociality did not reach statistical significance.

The same pattern emerged in summer: medium- and high-sociality individuals showed significantly higher survival probabilities (0.72 [0.50, 0.88] and 0.66 [0.42, 0.85], respectively) than low-sociality individuals (0.51 [0.27, 0.74]; Figure 5, Tables S5 and S6). The posterior median differences were 0.21 for medium vs. low and 0.15 for high

vs. low. Survival probabilities did not differ significantly between medium- and high-sociality individuals.

During the winter period, we found no evidence for differences in survival associated with sex (β_{Sex_w}= 0.30[−0.24, 0.86]) or age (β_{Age_w}= 0.06[−0.07,0.24]). During the summer period, females showed lower survival than males (β_{Sex_s}= −0.62[−1.04, −0.20]), whereas no evidence for an effect of age was detected (β_{Age_s}= 0.02[−0.08, 0.12].

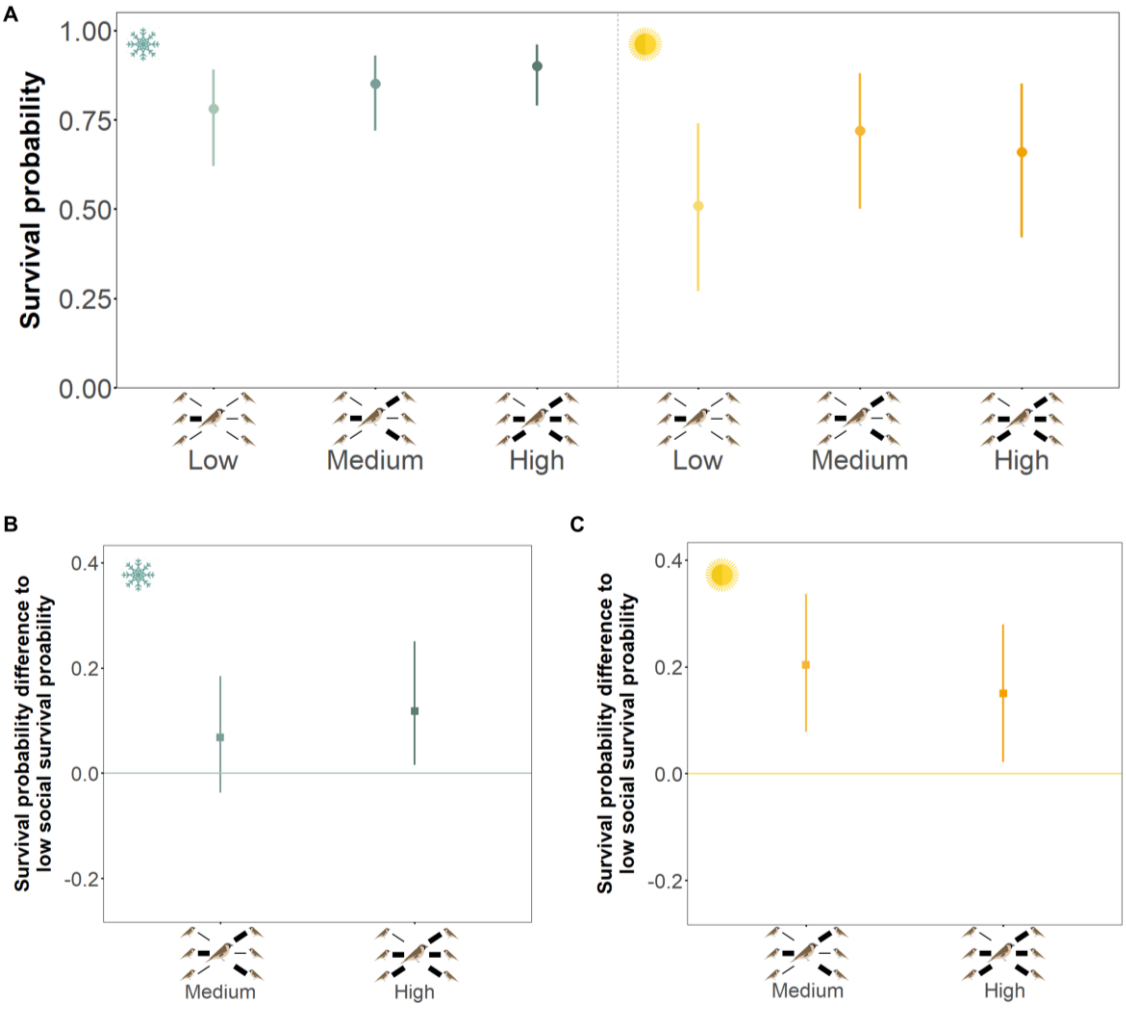

Figure 5. Survival probabilities. A) Model estimates of survival probabilities for low, medium and high sociality individuals for winter and summer intervals. Dots represent the posterior mean estimates and bars their 95% credible intervals. **B)** and **C)** Posterior mean differences in survival probabilities between low sociality individuals and medium

and high sociality individuals for winter and summer, respectively. Squares represent the mean differences, and bars indicate the 95% credible intervals of the differences.

Sensitivity analysis of the strong-bond threshold

Results were qualitatively robust to alternative definitions of strong social bonds (70% and 90% thresholds). Across thresholds, detection probabilities did not differ between sociality categories, and the overall structure of state transitions was broadly preserved. For survival, high- and medium-sociality individuals consistently showed higher survival than low-sociality individuals in both winter and summer across all thresholds. Although the statistical support of a few specific pairwise contrasts varied slightly depending on the threshold used, the overall biological pattern—higher survival associated with greater sociality—remained stable (Supplementary Tables S8–S13).

DISCUSSION

Our results show that sociable weavers show a moderate repeatability in individual sociality levels, which are based on their number of strong social bonds. Furthermore, individuals with medium and high sociality levels exhibited a higher survival probability than those with a lower sociality. These findings suggest that, in our population, more social individuals experience a survival advantage that could increase their overall fitness. Importantly, by incorporating state-dependent individual detectability, our model accounted for differences in detection probability across sociality levels, ensuring that

observed variation in survival reflects biological differences rather than methodological artefacts.

Consistency of individual sociality across years

We found that transitions in sociality were structured rather than random. For all categories, remaining in the same sociality state was the most likely individual outcome, although for low- and medium-sociality individuals the combined probability of transitioning to other categories was similar to that of remaining in the same one. When transitions occurred, they tended to be between adjacent categories, with transitions between extremes being least likely. High-sociality individuals showed the strongest consistency, with a higher probability of remaining in the same category than transitioning overall, whereas low-sociality individuals showed weaker consistency, as the probability of remaining low did not differ significantly from transitioning to medium (Figure 4, Table S6).

To complement transition probabilities with a formal measure of temporal consistency, we estimated repeatability of sociality level and found moderate among-individual consistency across years. This estimate is broadly consistent with repeatability values reported for individual-level social network metrics (e.g. degree, strength, betweenness centrality, and closeness) in other systems, including birds (Aplin et al., 2015; Dunning et al., 2023; Plaza et al., 2020) and mammals (Blumstein et al., 2013; Vander Wal et al., 2015), which often fall in a similar range (approximately 0.2–0.6, depending on the metric and timescale). Work using other approaches also supports temporal stability in social structure and individual network position (e.g. across-year network stability or rank-order

concordance in birds and fish; (Jacoby et al., 2014; S. Krause et al., 2017; Shizuka et al., 2014).

While overall results support temporal consistency in individual sociality, they also suggest weaker stability in low-sociality individuals. Specifically, the probability of remaining low did not differ significantly from that of transitioning to medium (Figure 4, Tables S5 and S6), and only differed from transitions to high sociality. This contrasts with the stronger stability observed in medium- and high-sociality individuals. This weaker stability may reflect life-stage changes that alter opportunities to form strong bonds, consistent with the slight increase in sociality with age detected in the repeatability model. Some low-sociality individuals may also increase their number of strong social bonds over time—potentially through social niche construction (Trappes et al., 2022)— which could increase access to benefits associated with stronger bonding, such as higher survival. Testing this possibility will require future work that directly quantifies the behavioural processes underlying bond formation and turnover. At the same time, variation in sociality within individuals over time suggests that its expression is influenced by changes in the social environment, including changes in group composition driven by mortality, dispersal, or fluctuations in colony size (Schradin, 2013), as well as by the identity and behaviour of social partners (Niemelä & Santostefano, 2015).

Despite this, the observed consistency in individual sociality underscores its potential to evolve in sociable weavers. Temporal consistency is not a strict requirement for evolution, but it can increase the scope for selection by ensuring that among-individual differences are repeatedly expressed and can thus be consistently associated with fitness outcomes (Boake, 1989). This is particularly relevant for sociality, which depends not only on individual traits but also on the social environment. If the expression of a social metric is dominated by stochastic environmental or social fluctuations, directional

selection is expected to be less effective, reducing the likelihood or rate of evolutionary change even when the trait has strong fitness consequences.

Individuals with higher sociality show increased survival

We found that individuals with medium and high sociality (reflecting their relatively higher number of strong social bonds) tended to show higher survival probabilities than low-sociality individuals. This pattern was observed in both winter (July–August, where the difference was statistically supported only for high-sociality individuals) and summer (October–March, where both medium- and high-sociality individuals differed significantly from low-sociality individuals). The recurrence of this pattern across seasons suggests that the association between sociality and survival is not restricted to a single seasonal context and may reflect persistent or season-specific mechanisms, or a combination of both. Because sociality categories were defined relative to the distribution of strong bonds within each colony-year, our results indicate that individuals with a greater number of strong social bonds than others in the same colony-year tend to experience higher survival. This is consistent with previous studies showing positive associations between sociality and survival across a range of taxa (Archie et al., 2014; Barocas et al., 2011; Blumstein et al., 2013; Campos et al., 2020; Lehmann et al., 2016; Silk et al., 2010; Stanton & Mann, 2012; Thompson & Cords, 2018).

Although sociable weavers generally forage in cohesive colony groups—expected to provide foraging benefits to all members (Brown et al., 2003; Lloyd et al., 2018)—highly social individuals may gain additional advantages through nepotistic behaviours from group members (Rat, 2015). Specifically, individuals may receive preferential access to food shared within their social group (Chiarati et al., 2011; Ekman et al., 2000), or benefit

525 from enhanced information-sharing about novel food sources, which facilitates their
526 discovery and exploitation (McMahon et al., 2024). Additionally, highly social
527 individuals may experience nepotistic protection from predators, further increasing their
528 survival (Griesser & Ekman, 2004, 2005). Finally, being part of a larger and more
529 cohesive group may reduce harassment from conspecifics, thereby lowering energy
530 expenditure and stress (Cameron et al., 2009).

531 During winter, thermoregulatory benefits associated with access to roosting chambers and
532 communal roosting are likely to play a crucial role in improving condition and survival.
533 In sociable weavers, the communal nest provides significant insulation (Lowney et al.,
534 2020; White et al., 1975), and night-time nest chamber temperatures are positively
535 correlated with the number of birds roosting together, especially on cold nights (Paquet
536 et al., 2016). Birds in larger roosting groups are therefore less exposed to extreme cold.
537 If sociality influences group composition at night, medium- and high-social individuals
538 may be more likely to roost in larger groups and thus benefit from improved
539 thermoregulation, reduced energy expenditure, and lower risk of cold-related mortality.

540 Survival benefits may also be linked to cooperative breeding behaviours. In sociable
541 weavers, helpers-at-the-nest tend to form stronger social bonds with breeders and other
542 breeding group members (Ferreira et al., 2020, 2024), and younger females with more
543 helpers showed higher survival (Paquet et al., 2015). This pattern is likely due to reduced
544 parental effort (Hatchwell, 1999), and similar patterns are found in other cooperative
545 breeders (Downing et al., 2021). This benefit may also extend to helpers, since helping
546 incurs physiological costs, particularly under high effort (Covas et al., 2022). If individual
547 sociality (i.e., number of strong bonds) were positively associated with the number of
548 helpers received (Ferreira et al., 2024) and the amount of help provided (Covas et al.,
549 2008), higher sociality individuals could experience increased survival. However,

ongoing work by our group indicates that the number of strong social bonds is not associated with the number of helpers present at the nest (Spearman's $\rho \approx 0$ in both sexes; Munar-Delgado et al., in preparation).

Moreover, the number of strong social bonds typically exceeds the average number of helpers within breeding groups in our population (mean breeding group size = 3.15; Covas et al., 2006). Hence, while breeder–helper relationships could still contribute to the association between sociality and survival, the association found here between the number of strong social bonds and survival is unlikely to be explained by a third association with the number of helpers. Further understanding the association between individual sociality and cooperative breeding, and whether interactions between these two components of social life affect fitness, will require additional work explicitly integrating reproductive roles with social network metrics.

As our study is observational, we cannot exclude the possibility that third variables contribute to the observed association between sociality and apparent survival. One possibility is that underlying differences in individual health generate a correlation between sociality and survival, for example through infection-induced behavioural changes that reduce social connectivity while simultaneously increasing mortality risk (Lopes et al., 2016). However, infection processes could also disproportionately affect highly social individuals, who experience higher contact rates and therefore greater exposure to pathogens (VanderWaal et al., 2014), potentially leading to reduced survival or greater instability in sociality in this category. In contrast, highly social individuals in our population often remained in the high sociality category across years, rather than showing the increased transitions to lower sociality that would be expected if infection-driven processes were driving the pattern.

Another non-causal explanation is age-related senescence, whereby older individuals progressively lose social connections as a consequence of declining condition (Albery et al., 2022), while also experiencing reduced survival. Age was explicitly accounted for in our models, and the association between sociality and apparent survival persisted after controlling for age, making it unlikely that age-related declines in sociality alone explain the observed pattern.

Sociality may also reflect broader differences in individual quality or in the social or ecological environments individuals experience, rather than exerting a direct effect on survival. For example, individuals in better condition may both survive better and be able to maintain a greater number of strong social bonds, generating a correlation between sociality and survival without direct causation. As in most observational studies, experimental approaches that manipulate social opportunities would be required to establish causality unambiguously.

Finally, a methodological limitation of our analyses is that the multi-state capture–recapture model estimates apparent survival, which conflates true mortality with permanent emigration. This is particularly relevant in sociable weavers, where dispersal is strongly female-biased (van Dijk et al., 2015), and likely contributes to the lower apparent survival observed in females during the summer period. Importantly, sociality remained a significant predictor of apparent survival after accounting for sex and age, and showed a consistent effect across seasons, suggesting that the observed association is unlikely to be driven solely by sex-biased dispersal.

Together, our results indicate that individual sociality is both moderately consistent and associated with survival, suggesting that it may be subject to directional selection in this

population. However, survival alone does not capture lifetime reproductive output and establishing causality and evaluating net selection on sociality will require integrating additional fitness components (e.g. reproduction or lifetime reproductive success) and, where possible, approaches that disentangle mortality from permanent emigration. Assessing its evolutionary potential will also require quantifying the relative contributions of genetic and environmental sources of variation, including the role of indirect genetic effects arising from social interactions (Moore et al., 1997; Wolf et al., 1998), as well as the potential for gene–environment correlations in socially structured populations (Munar-Delgado et al., 2023). At the same time, the persistence of variation in sociality despite its apparent survival benefits suggests that it may be maintained by trade-offs with other fitness components or by context-dependent selection (Montiglio et al., 2013). For example, high sociality might be associated with delayed onset of breeding due to greater investment in social relationships, increased competition for breeding opportunities, or higher susceptibility to disease during outbreaks, which could offset these survival benefits. Future work should aim to identify the genetic and environmental sources of variation in sociality, as well as the mechanisms linking sociality and survival—for example, by manipulating social opportunities through restricted access to automated feeders (Firth et al., 2016; Heinen et al., 2022)—and to assess potential trade-offs with other fitness components.

ACKNOWLEDGEMENTS

We thank Annie Basson for her help building the RFID stations and all the field workers that helped collecting the data: Louis Bliard, Corisande Abiven, Tshianeo Melda, Lesego Moagi, Natasha Prindal, Paola Stefanini , Irene Baquero, Taylor Keet, and all persons who helped with the annual captures. De Beers Consolidated Mines provided access to Benfontein Reserve. This study was funded by an ERC Consolidator grant 866489 (EU) to R.C. and the ANR 19CE02-0014-01 OSU OREME and SEE-Life (CNRS, France) to CD. RC was funded by FCT (CEECIND/03451/2018).

AUTHOR CONTRIBUTIONS

RC, CL and AF conceived and designed the study. GM-D, MP, AF and BF developed the methodology. RC, CD, AF, BF and FT collected the data. GM-D, MP and AF implemented the software; GM-D and BF curated the data. GM-D and MP conducted the formal analyses; GM-D created the visualizations. RC and CD acquired funding, provided resources, and supervised the project. GM-D wrote the original draft, and all authors contributed substantially to revising the manuscript.

ETHICAL STATEMENT

Birds were captured and handled in accordance with protocols approved by Northern Cape Nature Conservation (permits FAUNA 1338/2017, 0684/2019, 0059/2021, and 0775/2023) and the Ethics Committee of the University of Cape Town (2014/V1/RC, 2018/V20/RC, 2020/2018/V22/RC/A1, and 2023/V8/RC). All efforts were made to

644 minimize handling time and disturbance, and to ensure that procedures caused the least
645 possible stress to the animals.

646

647 **DATA AVAILABILITY STATEMENT**

648 Data (https://doi.org/10.5281/zenodo.16276322) and codes
649 (https://doi.org/10.5281/zenodo.16276060). are available at Zenodo

650

651 **REFERENCES**

652 Albery, G. F., Clutton-Brock, T. H., Morris, A., Morris, S., Pemberton, J. M., Nussey,
653 D. H., & Firth, J. A. (2022). Ageing red deer alter their spatial behaviour and
654 become less social. *Nature Ecology & Evolution*, *6*(8), 1231–1238.
655 https://doi.org/10.1038/s41559-022-01817-9
656 Aplin, L. M., Farine, D. R., Morand-Ferron, J., & Sheldon, B. C. (2012). Social
657 networks predict patch discovery in a wild population of songbirds. *Proceedings*
658 *of the Royal Society B: Biological Sciences*, *279*(1745), 4199–4205.
659 https://doi.org/10.1098/rspb.2012.1591
660 Aplin, L. M., Firth, J. A., Farine, D. R., Voelkl, B., Crates, R. A., Culina, A., Garroway,
661 C. J., Hinde, C. A., Kidd, L. R., Psorakis, I., Milligan, N. D., Radersma, R.,
662 Verhelst, B. L., & Sheldon, B. C. (2015). Consistent individual differences in
663 the social phenotypes of wild great tits, *Parus major*. *Animal Behaviour*, *108*,
664 117–127. https://doi.org/10.1016/j.anbehav.2015.07.016
665 Archie, E. A., Tung, J., Clark, M., Altmann, J., & Alberts, S. C. (2014). Social
666 affiliation matters: Both same-sex and opposite-sex relationships predict

667 survival in wild female baboons. *Proceedings of the Royal Society B: Biological*
668 *Sciences*, *281*(1793), 20141261. https://doi.org/10.1098/rspb.2014.1261
669 Barocas, A., Ilany, A., Koren, L., Kam, M., & Geffen, E. (2011). Variance in Centrality
670 within Rock Hyrax Social Networks Predicts Adult Longevity. *PLOS ONE*,
671 *6*(7), e22375. https://doi.org/10.1371/journal.pone.0022375
672 Bilde, T., Coates, K. S., Birkhofer, K., Bird, T., Maklakov, A. A., Lubin, Y., & Avilés,
673 L. (2007). Survival benefits select for group living in a social spider despite
674 reproductive costs. *Journal of Evolutionary Biology*, *20*(6), 2412–2426.
675 https://doi.org/10.1111/j.1420-9101.2007.01407.x
676 Blumstein, D. T., Petelle, M. B., & Wey, T. W. (2013). Defensive and social
677 aggression: Repeatable but independent. *Behavioral Ecology*, *24*(2), 457–461.
678 https://doi.org/10.1093/beheco/ars183
679 Boake, C. R. B. (1989). Repeatability: Its role in evolutionary studies of mating
680 behavior. *Evolutionary Ecology*, *3*(2), Article 2.
681 https://doi.org/10.1007/BF02270919
682 Brown, C. R., Covas, R., Anderson, M. D., & Brown, M. B. (2003). Multistate
683 estimates of survival and movement in relation to colony size in the sociable
684 weaver. *Behavioral Ecology*, *14*(4), 463–471.
685 https://doi.org/10.1093/beheco/arg034
686 Bürkner, P.-C. (2017). brms: An R Package for Bayesian Multilevel Models Using Stan.
687 *Journal of Statistical Software*, *80*, 1–28. https://doi.org/10.18637/jss.v080.i01
688 Camerlenghi, E., McQueen, A., Delhey, K., Cook, C. N., Kingma, S. A., Farine, D. R.,
689 & Peters, A. (2022). Cooperative breeding and the emergence of multilevel
690 societies in birds. *Ecology Letters*, *25*(4), 766–777.
691 https://doi.org/10.1111/ele.13950

692 Cameron, E. Z., Setsaas, T. H., & Linklater, W. L. (2009). Social bonds between
693 unrelated females increase reproductive success in feral horses. *Proceedings of*
694 *the National Academy of Sciences of the United States of America*, *106*(33),
695 13850–13853. https://doi.org/10.1073/pnas.0900639106
696 Campbell, L. A. D., Tkaczynski, P. J., Lehmann, J., Mouna, M., & Majolo, B. (2018).
697 Social thermoregulation as a potential mechanism linking sociality and fitness:
698 Barbary macaques with more social partners form larger huddles. *Scientific*
699 *Reports*, *8*(1), 6074. https://doi.org/10.1038/s41598-018-24373-4
700 Campos, F. A., Villavicencio, F., Archie, E. A., Colchero, F., & Alberts, S. C. (2020).
701 Social bonds, social status and survival in wild baboons: A tale of two sexes.
702 *Philosophical Transactions of the Royal Society B: Biological Sciences*,
703 *375*(1811), 20190621. https://doi.org/10.1098/rstb.2019.0621
704 Chiarati, E., Canestrari, D., Vila, M., Vera, R., & Baglione, V. (2011). Nepotistic access
705 to food resources in cooperatively breeding carrion crows. *Behavioral Ecology*
706 *and Sociobiology*, *65*(9), Article 9. https://doi.org/10.1007/s00265-011-1187-1
707 Covas, R., Dalecky, A., Caizergues, A., & Doutrelant, C. (2006). Kin associations and
708 direct vs indirect fitness benefits in colonial cooperatively breeding sociable
709 weavers Philetairus socius. *Behavioral Ecology and Sociobiology*, *60*(3), 323–
710 331. https://doi.org/10.1007/s00265-006-0168-2
711 Covas, R., du Plessis, M. A., & Doutrelant, C. (2008). Helpers in colonial cooperatively
712 breeding sociable weavers Philetairus socius contribute to buffer the effects of
713 adverse breeding conditions. *Behavioral Ecology and Sociobiology*, *63*(1), 103–
714 112. https://doi.org/10.1007/s00265-008-0640-2
715 Covas, R., Lardy, S., Silva, L. R., Rey, B., Ferreira, A. C., Theron, F., Tognetti, A.,
716 Faivre, B., & Doutrelant, C. (2022). The oxidative cost of helping and its

minimization in a cooperative breeder. *Behavioral Ecology*, *33*(3), 504–517. https://doi.org/10.1093/beheco/arab152

De Moor, D., & Brent, L. J. N. (2025). Quality, quantity, and the adaptive function of social relationships. *Trends in Ecology & Evolution*, *40*(12), 1199–1211. https://doi.org/10.1016/j.tree.2025.09.004

De Valpine, P., Turek, D., Paciorek, C. J., Anderson-Bergman, C., Lang, D. T., & Bodik, R. (2017). Programming with models: Writing statistical algorithms for general model structures with NIMBLE. *Journal of Computational and Graphical Statistics*, *26*(2), 403–413. https://doi.org/10.1080/10618600.2016.1172487

Downing, P. A., Griffin, A. S., & Cornwallis, C. K. (2021). Hard-working helpers contribute to long breeder lifespans in cooperative birds. *Philosophical Transactions of the Royal Society B: Biological Sciences*, *376*(1823), 20190742. https://doi.org/10.1098/rstb.2019.0742

Dunning, J., Burke, T., Hoi Hang Chan, A., Ying Janet Chik, H., Evans, T., & Schroeder, J. (2023). Opposite-sex associations are linked with annual fitness, but sociality is stable over lifetime. *Behavioral Ecology*, *34*(3), 315–324. https://doi.org/10.1093/beheco/arac124

Ekman, J., Bylin, A., & Tegelström, H. (2000). Parental nepotism enhances survival of retained offspring in the Siberian jay. *Behavioral Ecology*, *11*(4), 416–420. https://doi.org/10.1093/beheco/11.4.416

Ellis, S., Franks, D. W., Nattrass, S., Cant, M. A., Weiss, M. N., Giles, D., Balcomb, K. C., & Croft, D. P. (2017). Mortality risk and social network position in resident killer whales: Sex differences and the importance of resource abundance.

Proceedings of the Royal Society B: Biological Sciences, *284*(1865), 20171313. https://doi.org/10.1098/rspb.2017.1313

Ellis, S., Snyder-Mackler, N., Ruiz-Lambides, A., Platt, M. L., & Brent, L. J. N. (2019). Deconstructing sociality: The types of social connections that predict longevity in a group-living primate. *Proceedings of the Royal Society B: Biological Sciences*, *286*(1917), 20191991. https://doi.org/10.1098/rspb.2019.1991

Evans, T., Krzyszczyk, E., Frère, C., & Mann, J. (2021). Lifetime stability of social traits in bottlenose dolphins. *Communications Biology*, *4*(1), 1–8. https://doi.org/10.1038/s42003-021-02292-x

Ferreira, A. C., Covas, R., Silva, L. R., Esteves, S. C., Duarte, I. F., Fortuna, R., Theron, F., Doutrelant, C., & Farine, D. R. (2020). How to make methodological decisions when inferring social networks. *Ecology and Evolution*, *10*(17), 9132–9143. https://doi.org/10.1002/ece3.6568

Ferreira, A. C., Farine, D. R., Silva, L. R., Fortuna, R., Doutrelant, C., & Covas, R. (2024). *Foraging associations are related with helping interactions in a cooperatively breeding bird* (p. 2024.10.28.620677). bioRxiv. https://doi.org/10.1101/2024.10.28.620677

Firth, J. A., Sheldon, B. C., & Farine, D. R. (2016). Pathways of information transmission among wild songbirds follow experimentally imposed changes in social foraging structure. *Biology Letters*, *12*(6), 20160144. https://doi.org/10.1098/rsbl.2016.0144

Formica, V. A., Wood, C. W., Larsen, W. B., Butterfield, R. E., Augat, M. E., Hougen, H. Y., & Brodie, E. D., III. (2012). Fitness consequences of social network position in a wild population of forked fungus beetles (Bolitotherus cornutus).

765 *Journal of Evolutionary Biology*, *25*(1), 130–137.
766 https://doi.org/10.1111/j.1420-9101.2011.02411.x
767 Gelman, A., & Rubin, D. B. (1992). Inference from Iterative Simulation Using Multiple
768 Sequences. *Statistical Science*, *7*(4), 457–472.
769 https://doi.org/10.1214/ss/1177011136
770 Gero, S., Bejder, L., Whitehead, H., Mann, J., & Connor, R. C. (2005). Behaviourally
771 specific preferred associations in bottlenose dolphins, Tursiops spp. *Canadian*
772 *Journal of Zoology*, *83*(12), 1566–1573. https://doi.org/10.1139/z05-155
773 Ginsberg, J. R., & Young, T. P. (1992). Measuring association between individuals or
774 groups in behavioural studies. *Animal Behaviour*, *44*, 377–379.
775 https://doi.org/10.1016/0003-3472(92)90042-8
776 Griesser, M., & Ekman, J. (2004). Nepotistic alarm calling in the Siberian jay,
777 *Perisoreus infaustus*. *Animal Behaviour*, *67*(5), 933–939.
778 https://doi.org/10.1016/j.anbehav.2003.09.005
779 Griesser, M., & Ekman, J. (2005). Nepotistic mobbing behaviour in the Siberian jay,
780 *Perisoreus infaustus*. *Animal Behaviour*, *69*(2), 345–352.
781 https://doi.org/10.1016/j.anbehav.2004.05.013
782 Hatchwell, B. J. (1999). Investment Strategies of Breeders in Avian Cooperative
783 Breeding Systems. *The American Naturalist*, *154*(2), 205–219.
784 https://doi.org/10.1086/303227
785 Heinen, V. K., Benedict, L. M., Sonnenberg, B. R., Bridge, E. S., Farine, D. R., &
786 Pravosudov, V. V. (2022). Experimental manipulation of food distribution alters
787 social networks and information transmission across environments in a food-
788 caching bird. *Animal Behaviour*, *193*, 1–12.
789 https://doi.org/10.1016/j.anbehav.2022.08.007

790 Jacoby, D. M. P., Fear, L. N., Sims, D. W., & Croft, D. P. (2014). Shark personalities?
791 Repeatability of social network traits in a widely distributed predatory fish.
792 *Behavioral Ecology and Sociobiology*, *68*(12), Article 12.
793 https://doi.org/10.1007/s00265-014-1805-9
794 Kern, J. M., & Radford, A. N. (2021). Strongly bonded individuals prefer to forage
795 together in cooperatively breeding dwarf mongoose groups. *Behavioral Ecology*
796 *and Sociobiology*, *75*(5), 85. https://doi.org/10.1007/s00265-021-03025-0
797 Koenig, W. D. (1981). Reproductive Success, Group Size, and the Evolution of
798 Cooperative Breeding in the Acorn Woodpecker. *The American Naturalist*,
799 *117*(4), 421–443. https://doi.org/10.1086/283726
800 Krause, J., Ruxton, G. D., Krause, J., & Ruxton, G. D. (2002). *Living in Groups*. Oxford
801 University Press.
802 Krause, S., Wilson, A. D. M., Ramnarine, I. W., Herbert-Read, J. E., Clément, R. J. G.,
803 & Krause, J. (2017). Guppies occupy consistent positions in social networks:
804 Mechanisms and consequences. *Behavioral Ecology*, *28*(2), 429–438.
805 https://doi.org/10.1093/beheco/arw177
806 Lebreton, J. D., & Cefe, R. P. (2002). Multistate recapture models: Modelling
807 incomplete individual histories. *Journal of Applied Statistics*, *29*(1–4), 353–369.
808 https://doi.org/10.1080/02664760120108638
809 Lebreton, J., Nichols, J. D., Barker, R. J., Pradel, R., & Spendelow, J. A. (2009).
810 Chapter 3 Modeling Individual Animal Histories with Multistate Capture–
811 Recapture Models. In *Advances in Ecological Research* (Vol. 41, pp. 87–173).
812 Academic Press. https://doi.org/10.1016/S0065-2504(09)00403-6

Lehmann, J., Majolo, B., & McFarland, R. (2016). The effects of social network position on the survival of wild Barbary macaques, Macaca sylvanus. *Behavioral Ecology*, *27*(1), 20–28. https://doi.org/10.1093/beheco/arv169

Lloyd, K. J., Altwegg, R., Doutrelant, C., & Covas, R. (2018). Factors affecting the foraging distance and duration of a colonial bird, the sociable weaver, in a semi-arid environment. *African Journal of Ecology*, *56*(3), 659–663. https://doi.org/10.1111/aje.12484

Lopes, P. C., Block, P., & König, B. (2016). Infection-induced behavioural changes reduce connectivity and the potential for disease spread in wild mice contact networks. *Scientific Reports*, *6*(1), 31790. https://doi.org/10.1038/srep31790

Lowney, A. M., Bolopo, D., Krochuk, B. A., & Thomson, R. L. (2020). The Large Communal Nests of Sociable Weavers Provide Year-Round Insulated Refuge for Weavers and Pygmy Falcons. *Frontiers in Ecology and Evolution*, *8*. https://doi.org/10.3389/fevo.2020.570006

Maclean, G. L. (1973). The Sociable Weaver, Part 2: Nest Architecture and Social Organization. *Ostrich*, *44*(3–4), 191–218. https://doi.org/10.1080/00306525.1973.9639159

Marshall, H. H., Carter, A. J., Ashford, A., Rowcliffe, J. M., & Cowlishaw, G. (2015). Social effects on foraging behavior and success depend on local environmental conditions. *Ecology and Evolution*, *5*(2), 475–492. https://doi.org/10.1002/ece3.1377

Martin, T. E. (1995). Avian Life History Evolution in Relation to Nest Sites, Nest Predation, and Food. *Ecological Monographs*, *65*(1), 101–127. https://doi.org/10.2307/2937160

McMahon, K., Marples, N. M., Spurgin, L. G., Rowland, H. M., Sheldon, B. C., & Firth, J. A. (2024). Social network centrality predicts dietary decisions in a wild bird population. *iScience*, *27*(5). https://doi.org/10.1016/j.isci.2024.109581

Montiglio, P.-O., Ferrari, C., & Réale, D. (2013). Social niche specialization under constraints: Personality, social interactions and environmental heterogeneity. *Philosophical Transactions of the Royal Society B: Biological Sciences*, *368*(1618), 20120343. https://doi.org/10.1098/rstb.2012.0343

Moore, A. J., III Brodie, E. D., & Wolf, J. B. (1997). Interacting phenotypes and the evolutionary process: I. Direct and indirect genetic effects of social interactions. *Evolution*, *51*(5), 1352–1362. https://doi.org/10.1111/j.1558-5646.1997.tb01458.x

Munar-Delgado, G., Araya-Ajoy, Y. G., & Edelaar, P. (2023). Estimation of additive genetic variance when there are gene–environment correlations: Pitfalls, solutions and unexplored questions. *Methods in Ecology and Evolution*, *14*(5), 1245–1258. https://doi.org/10.1111/2041-210X.14098

Nakagawa, S., & Schielzeth, H. (2013). A general and simple method for obtaining R2 from generalized linear mixed-effects models. *Methods in Ecology and Evolution*, *4*(2), 133–142. https://doi.org/10.1111/j.2041-210x.2012.00261.x

Niemelä, P. T., & Santostefano, F. (2015). *Social carry-over effects on non-social behavioral variation: Mechanisms and consequences*. https://www.frontiersin.org/journals/ecology-and-evolution/articles/10.3389/fevo.2015.00049/full#B49

NIMBLE Development Team. (2025). *NIMBLE: MCMC, Particle Filtering, and Programmable Hierarchical Modeling* (Version 1.4.0) [Computer software]. Zenodo. https://doi.org/10.5281/ZENODO.1211190

Pacheco, L. (2022). *Roosting dynamics: Assessing the "pay-to-stay" hypothesis using a social network approach* [MSc thesis]. Universidade do Porto.

Paquet, M., Doutrelant, C., Hatchwell, B. J., Spottiswoode, C. N., & Covas, R. (2015). Antagonistic effect of helpers on breeding male and female survival in a cooperatively breeding bird. *Journal of Animal Ecology*, *84*(5), 1354–1362. https://doi.org/10.1111/1365-2656.12377

Paquet, M., Doutrelant, C., Loubon, M., Theron, F., Rat, M., & Covas, R. (2016). Communal roosting, thermoregulatory benefits and breeding group size predictability in cooperatively breeding sociable weavers. *Journal of Avian Biology*, *47*(6), 749–755. https://doi.org/10.1111/jav.00916

Payevsky, V. A. (2021). Sex Ratio and Sex-Specific Survival in Avian Populations: A Review. *Biology Bulletin Reviews*, *11*(3), 317–327. https://doi.org/10.1134/S2079086421030099

Plaza, M., Burke, T., Cox, T., Flynn-Carroll, A., Girndt, A., Halford, G., Martin, D. A., Sanchez-Fortún, M., Sánchez-Tójar, A., Somerville, J., & Schroeder, J. (2020). Repeatable social network node-based metrics across populations and contexts in a passerine. *Journal of Evolutionary Biology*, *33*(11), 1634–1642. https://doi.org/10.1111/jeb.13703

R Core Team. (2020). *R: A language and environment for statistical computing* (Version 4.0.2) [Computer software]. https://www.R-project.org

Rat, M. E. T. (2015). *Dominance, social organisation and cooperation in the sociable weaver (Philetairus socius)* [PhD thesis]. http://hdl.handle.net/11427/16714

Schaub, M., Gimenez, O., Schmidt, B. R., & Pradel, R. (2004). Estimating Survival and Temporary Emigration in the Multistate Capture–Recapture Framework. *Ecology*, *85*(8), 2107–2113. https://doi.org/10.1890/03-3110

Schradin, C. (2013). Intraspecific variation in social organization by genetic variation, developmental plasticity, social flexibility or entirely extrinsic factors. *Philosophical Transactions of the Royal Society B: Biological Sciences*, *368*(1618), 20120346. https://doi.org/10.1098/rstb.2012.0346

Shizuka, D., Chaine, A. S., Anderson, J., Johnson, O., Laursen, I. M., & Lyon, B. E. (2014). Across-year social stability shapes network structure in wintering migrant sparrows. *Ecology Letters*, *17*(8), 998–1007. https://doi.org/10.1111/ele.12304

Silk, J. B., Beehner, J. C., Bergman, T. J., Crockford, C., Engh, A. L., Moscovice, L. R., Wittig, R. M., Seyfarth, R. M., & Cheney, D. L. (2010). Strong and Consistent Social Bonds Enhance the Longevity of Female Baboons. *Current Biology*, *20*(15), 1359–1361. https://doi.org/10.1016/j.cub.2010.05.067

Snyder-Mackler, N., Burger, J. R., Gaydosh, L., Belsky, D. W., Noppert, G. A., Campos, F. A., Bartolomucci, A., Yang, Y. C., Aiello, A. E., O'Rand, A., Harris, K. M., Shively, C. A., Alberts, S. C., & Tung, J. (2020). Social determinants of health and survival in humans and other animals. *Science*, *368*(6493), eaax9553. https://doi.org/10.1126/science.aax9553

Stanton, M. A., & Mann, J. (2012). *Early social networks predict Survival in wild bottlenose dolphins*. https://doi.org/10.1371/journal.pone.0047508

Testard, C., Shergold, C., Acevedo-Ithier, A., Hart, J., Bernau, A., Negron-Del Valle, J. E., Phillips, D., Watowich, M. M., Sanguinetti-Scheck, J. I., Montague, M. J., Snyder-Mackler, N., Higham, J. P., Platt, M. L., & Brent, L. J. N. (2024). Ecological disturbance alters the adaptive benefits of social ties. *Science*, *384*(6702), 1330–1335. https://doi.org/10.1126/science.adk0606

Thompson, N. A., & Cords, M. (2018). Stronger social bonds do not always predict greater longevity in a gregarious primate. *Ecology and Evolution*, *8*(3), 1604–1614. https://doi.org/10.1002/ece3.3781

Trappes, R., Nematipour, B., Kaiser, M. I., Krohs, U., van Benthem, K. J., Ernst, U. R., Gadau, J., Korsten, P., Kurtz, J., Schielzeth, H., Schmoll, T., & Takola, E. (2022). How individualized niches arise: Defining mechanisms of niche construction, niche choice, and niche conformance. *BioScience*, *72*(6), 538–548. https://doi.org/10.1093/biosci/biac023

van Dijk, R. E., Covas, R., Doutrelant, C., Spottiswoode, C. N., & Hatchwell, B. J. (2015). Fine-scale genetic structure reflects sex-specific dispersal strategies in a population of sociable weavers (Philetairus socius). *Molecular Ecology*, *24*(16), 4296–4311. https://doi.org/10.1111/mec.13308

Vander Wal, E., Festa-Bianchet, M., Réale, D., Coltman, D. W., & Pelletier, F. (2015). Sex-based differences in the adaptive value of social behavior contrasted against morphology and environment. *Ecology*, *96*(3), 631–641. https://doi.org/10.1890/14-1320.1

VanderWaal, K. L., Atwill, E. R., Isbell, Lynne. A., & McCowan, B. (2014). Linking social and pathogen transmission networks using microbial genetics in giraffe (Giraffa camelopardalis). *Journal of Animal Ecology*, *83*(2), 406–414. https://doi.org/10.1111/1365-2656.12137

White, F. N., Bartholomew, G. A., & Howell, T. R. (1975). The Thermal Significance of the Nest of the Sociable Weaver Philetairus Socius: Winter Observations. *Ibis*, *117*(2), 171–179. https://doi.org/10.1111/j.1474-919X.1975.tb04205.x

Wolf, J. B., Iii, E. D. B., Cheverud, J. M., Moore, A. J., & Wade, M. J. (1998). Evolutionary consequences of indirect genetic effects. *Trends in Ecology & Evolution*, *13*(2), 64–69. https://doi.org/10.1016/S0169-5347(97)01233-0

The number of strong social bonds is linked to survival in a cooperative bird

SUPPLEMENTARY MATERIAL

Parameters description as in Nimble code

Table S1. Description of parameters used in the Bayesian multi-state capture–recapture model, as implemented in Nimble. Notation used in the code, along with a brief explanation of each parameter's biological or modelling meaning.

Parameter	Description
phiLw	survival probability state L (Low sociality) during winter
phiMw	survival probability state M (Medium sociality) during winter
phiHw	survival probability state H (High sociality) during winter
phiLs	survival probability state L during summer
phiMs	survival probability state M during summer
phiHs	survival probability state H during summer
psiL[1]	transition probability from L to L, i.e. stay in state L
psiL[2]	transition probability from L to M
psiL[3]	transition probability from L to H
psiM[1]	transition probability from M to L
psiM[2]	transition probability from M to M i.e., stay in state M
psiM[3]	transition probability from M to H
psiH[1]	transition probability from H to L
psiH[2]	transition probability from H to M
psiH[3]	transition probability from H to H i.e. stay in stare H
pLn	recapture probability L at nets in sep
pMn	recapture probability M at nets in sep
pHn	recapture probability H at nets in sep
pLf	recapture probability L at feeders
pMf	recapture probability M at feeders
pHf	recapture probability H at feeders
betaLw	intercept of winter survival probability for state L (logit scale)
betaMw	intercept of winter survival probability for state M (logit scale)
betaHw	intercept of winter survival probability for state H (logit scale)
betaw[1]	coefficient for the effect of sex on winter survival probability
betaw[2]	coefficient for the effect of age on winter survival probability
epstw[]	random effect of year (t) on winter
epscw[]	random effect of colCNA on winter
betaLs	intercept of summer survival probability for state L (logit scale)
betaMs	intercept of summer survival probability for state M (logit scale)
betaHs	intercept of summer survival probability for state H (logit scale)
betas[1]	coefficient for the effect of sex on summer survival probability
betas[2]	coefficient for the effect of age on summer survival probability
epsts[]	random effect of year (t) on summer
epscs[]	random effect of colCNA on summer
betaDL	intercept of detection probability at RFID-feeders for state L (logit scale)
betaDM	intercept of detection probability at RFID-feeders for state M (logit scale)

betaDH	intercept of detection probability at RFID-feeders for state H (logit scale)
betaD	coefficient for the effect of RFID_at_Col on detection probability
age_centered	age matrix (in years)
sex_centered	centered sex vector
colCNA	colony matrix, represent to what colony each individual belonged each year
RFID_at_Col	matrix of RFID feeder presence at colonies

Specification of priors

Table S2. Specification of prior distributions used in the Bayesian multi-state capture–recapture model. Parameter notation corresponds to that described in Table S1. For each parameter, the prior distribution and its characteristics are provided.

Parameter	Prior	Description of prior values
psiL[1:3], psiM[1:3], psiH[1:3]	ddirch(alpha[1:3])	Dirichlet prior with concentration parameters 1, 1, 1 (i.e., equal weight to all transitions)
pln, pmn, phn	dunif(0, 1)	Uniform prior between 0 and 1 for detection probabilities
epstw[t], epsts[t]	dnorm(0, sd = sdepstw) dnorm(0, sd = sdepsts)	Normal prior with mean 0 and standard deviation sdepstw/ sdepsts
epscw[j], epscs[j]	dnorm(0, sd = sdepscw) dnorm(0, sd = sdepscs)	Normal prior with mean 0 and standard deviation sdepscw/sdepscs
sdepstw, sdepscw, sdepsts, sdepscs	dexp(1)	Exponential prior with rate 1
betaw[1], betaw[2]	dnorm(mean = 0, sd = 1.5)	Normal prior with mean 0 and standard deviation 1.5
betaLw, betaMw, betaHw	dnorm(mean = 0, sd = 1.5)	Normal prior with mean 0 and standard deviation 1.5
betas[1], betas[2]	dnorm(mean = 0, sd = 1.5)	Normal prior with mean 0 and standard deviation 1.5
betaLs, betaMs, betaHs	dnorm(mean = 0, sd = 1.5)	Normal prior with mean 0 and standard deviation 1.5

Model description

Table S3. Model equations used in the Bayesian multi-state capture–recapture analysis. All models used a logit link**.** Parameters are defined in Table S1 and priors in Table S2. See main text for rationale and code for implementation. *captured* is a dummy variable used to fix detection probability to 0 in 2020 due to missing RFID data.

	Model
Survival in winter	logit(phiLw[i,t]) <- betaLw + betaw[1] * sex_centered[i] + betaw[2] * age_centered[i,t] + epstw[t] + epscw[colCNA[i,t]]
	logit(phiMw[i,t]) <- betaMw + betaw[1] * sex_centered[i] + betaw[2] * age_centered[i,t] + epstw[t] + epscw[colCNA[i,t]]
	logit(phiLw[i,t]) <- betaLw + betaw[1] * sex_centered[i] + betaw[2] * age_centered[i,t] + epstw[t] + epscw[colCNA[i,t]]
Survival in summer and transitions	logit(phiLs[i,t]) <- betaLs + betas[1] * sex_centered[i] + betas[2] * age_centered[i,t] + epsts[t] + epscs[colCNA[i,t]]
	logit(phiMs[i,t]) <- betaMs + betas[1] * sex_centered[i] + betas[2] * age_centered[i,t] + epsts[t] + epscs[colCNA[i,t]]

	logit(phiHs[i,t]) <- betaHs + betas[1] * sex_centered[i] + betas[2] * age_centered[i,t] + epsts[t] + epscs[colCNA[i,t]]
Detection at RFIDs	logit(pLf[i,t]) <- (betaDL + betaD * RFID_at_Col[i,t]) * captured[t] - (1 - captured[t]) * 15
	logit(pMf[i,t]) <- (betaDM + betaD * RFID_at_Col[i,t]) * captured[t] - (1- captured[t]) * 15
	logit(pHf[i,t]) <- (betaDH + betaD * RFID_at_Col[i,t]) * captured[t] - (1- captured[t]) * 15

Covariates and random effects

- Age: For most birds (81%), we determined their exact age through breeding monitoring. For immigrant birds first captured as adults within the studied population (sociable weavers can disperse between colonies; (van Dijk et al., 2015), we estimated their age based on the average age of dispersal observed within our population. According to this, we assumed that immigrant individuals were 709 days old at the date of first capture (the average minimum dispersal age in our population; (Silva et al., 2025).

- Sex: During mist-nets samplings, individual blood samples were taken to determine sex through genetic sexing (Griffiths et al., 1998).

- Individual's colony: Birds were sometimes registered at RFID-feeder stations from different colonies. To assign each bird to a colony, we used mist-net sampling data, associating individuals with the colony where they were captured, which corresponds to their roosting location. If an individual was not captured at mist-nets in a specific year (*t*) but was registered at feeders, we used mist-net data from the following year to determine its colony identity. In cases where the individual was not captured the next year either, we relied on mist-net data from the previous year. Using this approach, we were able to assign a colony identity to every individual with social status data.

Individual exclusion criteria for multi-state capture–recapture analyses

We excluded individuals from the multi-state capture–recapture model based on three criteria. First, individuals were excluded if they only had RFID-feeder data from the last year of the study, as no recapture data could be obtained for them. Second, individuals for which sex could not be determined were excluded from the analysis, as sex was included as a covariate in the survival and transition components of the model. Third, only individuals from PIT-tagged colonies were retained. This is because social status estimates are calculated relative to the social structure of each colony, and individuals residing in non-tagged colonies could not be accurately assigned a social status. Individuals that ever migrated from PIT-tagged to non-tagged colonies were entirely excluded from the analysis, as their social status could not be determined after migration and the missing data could be wrongly interpreted by the model as mortality. Conversely, individuals that migrated from non-tagged to PIT-tagged colonies were retained, but only social status data from after migration were included.

Sociality levels classification

Table S4. Classification of sociality levels by year and colony. For each year-colony combination, the table shows the minimum and maximum numbers of strong social bonds observed within each category (see main text for classification criteria).

Year	Colony	Sociality level	Minimum strong bonds	Maximum strong bonds	Colony size at RFID-feeders
2018	11	Low	0	3	48
		Medium	4	7	
		High	8	16	
	20	Low	0	3	48
		Medium	4	7	
		High	8	16	
	27	Low	0	3	41
		Medium	4	8	
		High	9	16	
	43	Low	0	1	32
		Medium	2	6	
		High	7	11	
	71	Low	0	5	57
		Medium	6	10	
		High	11	24	
2019	11	Low	0	2	44
		Medium	3	6	
		High	7	12	
	20	Low	0	0	17
		Medium	1	2	
		High	3	4	
	27	Low	0	1	25
		Medium	2	3	
		High	4	9	
	43	Low	0	0	30
		Medium	1	1	
		High	2	6	
	71	Low	0	2	52
		Medium	3	4	
		High	5	12	
2021	11	Low	1	5	63
		Medium	6	10	
		High	11	16	
	20	Low	0	2	25
		Medium	3	7	
		High	8	10	
	27	Low	0	3	34
		Medium	4	8	
		High	9	15	

	43	Low	0	2	35
		Medium	3	4	
		High	5	9	
	71	Low	0	6	45
		Medium	7	8	
		High	9	19	
2022	11	Low	0	1	28
		Medium	2	5	
		High	6	11	
	20	Low	0	2	18
		Medium	3	3	
		High	4	6	
	21	Low	0	0	8
		Medium	1	1	
		High	2	2	
	71	Low	0	1	24
		Medium	2	4	
		High	5	10	
2023	11	Low	0	4	55
		Medium	5	12	
		High	13	23	
	20	Low	0	4	35
		Medium	5	8	
		High	9	20	
	21	Low	0	3	28
		Medium	4	5	
		High	6	9	
	71	Low	0	3	43
		Medium	4	9	
		High	10	15	

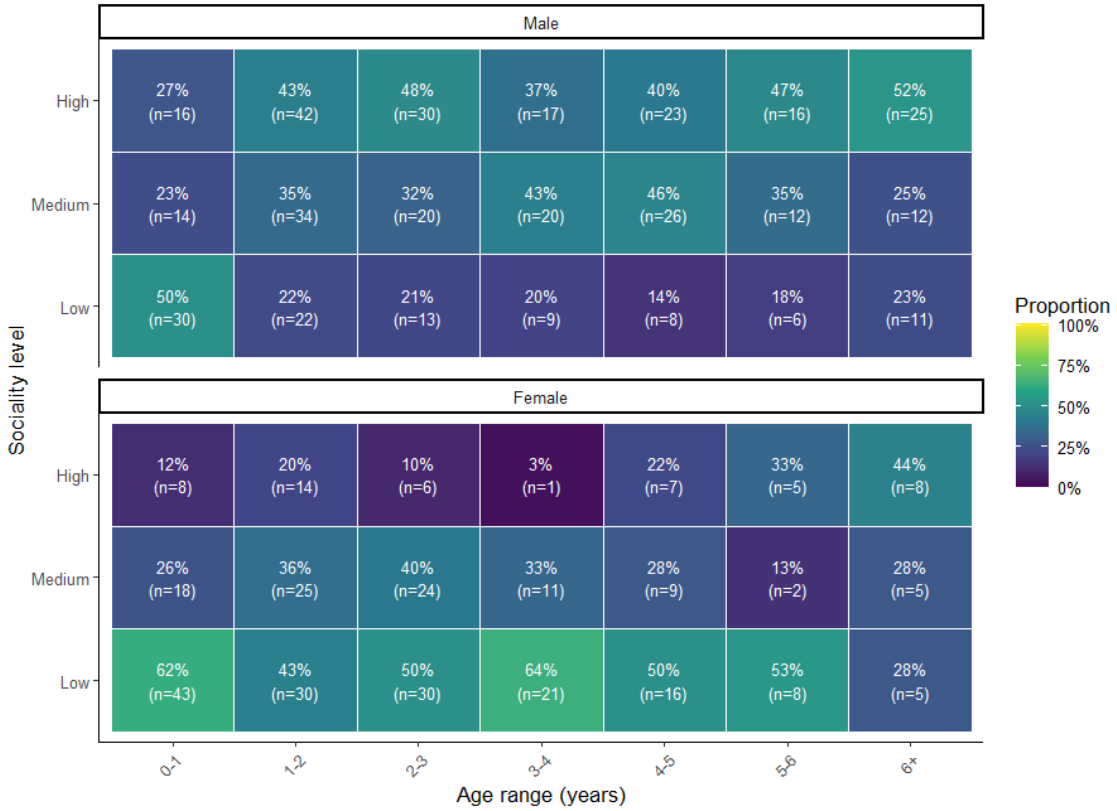

Figure S1. Descriptive overview of the distribution of observations across age classes, sexes, and sociality categories. Heatmaps show the proportion of observations classified as low, medium, or high sociality within each age class for males (top) and females (bottom). Numbers inside tiles indicate the proportion and sample size (n). Age classes are defined in one-year bins; individuals aged ≥6 years are grouped into a single category to avoid sparse cells and ensure adequate sample sizes.

Posterior predictive checks of the model

We assessed the goodness-of-fit of our model using Bayesian p-values (Gelman et al., 2014), a model-checking procedure that measures the dissimilarity between observed data and model predictions. We evaluated the dissimilarity between the observed and model-predicted means and coefficients of variation (CV) for the total number of re-detections per individual at mist nets and RFID-feeders. The reported Bayesian p-values indicate the proportion of simulated data generated from the model in which the distance between this simulated data and the expected mean (or CV) exceeds the distance between observed data and the expected mean (or CV). Values close to 0 or 1 (commonly below 0.05 or above 0.95) suggest a lack of fit.

To perform this analysis for detections at RFID-feeders, we transformed the observed data and model-prediction matrices (which contained four states: three social-status states and non-observation) into binomial matrices with observation (any social-status) and non-observation.

We obtain Bayesian p-values of 0.32 for mean of detections at the mist-nets, 0.49 for CV of detection at mist-nets, 0.26 for mean of detections at the RFID-feeders, 0.31 for CV of detection at RFID-feeders (Figure S2) showing no evidence for a lack of fit of our model to estimate the mean, and CV of the number of detections per individual.

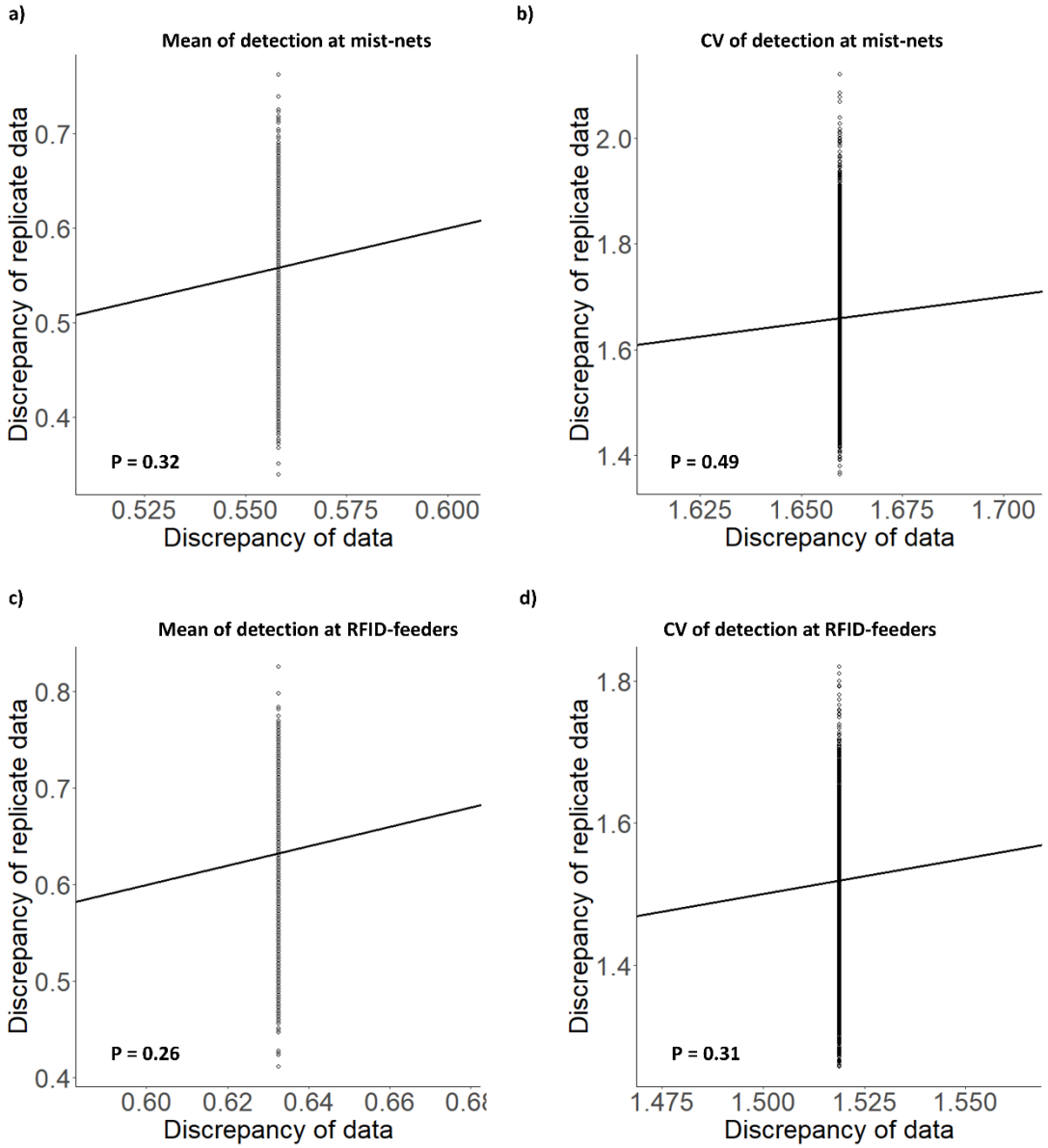

Figure S2. Posterior predictive checks of detection probabilities. P-values represent Bayesian p-values. a) Mean detection at mist-nets, b) coefficient of variation (CV) of detection at mist-nets, c) mean detection at RFID-feeders, and d) CV of detection at RFID-feeders.

Model convergence and mixing of chains

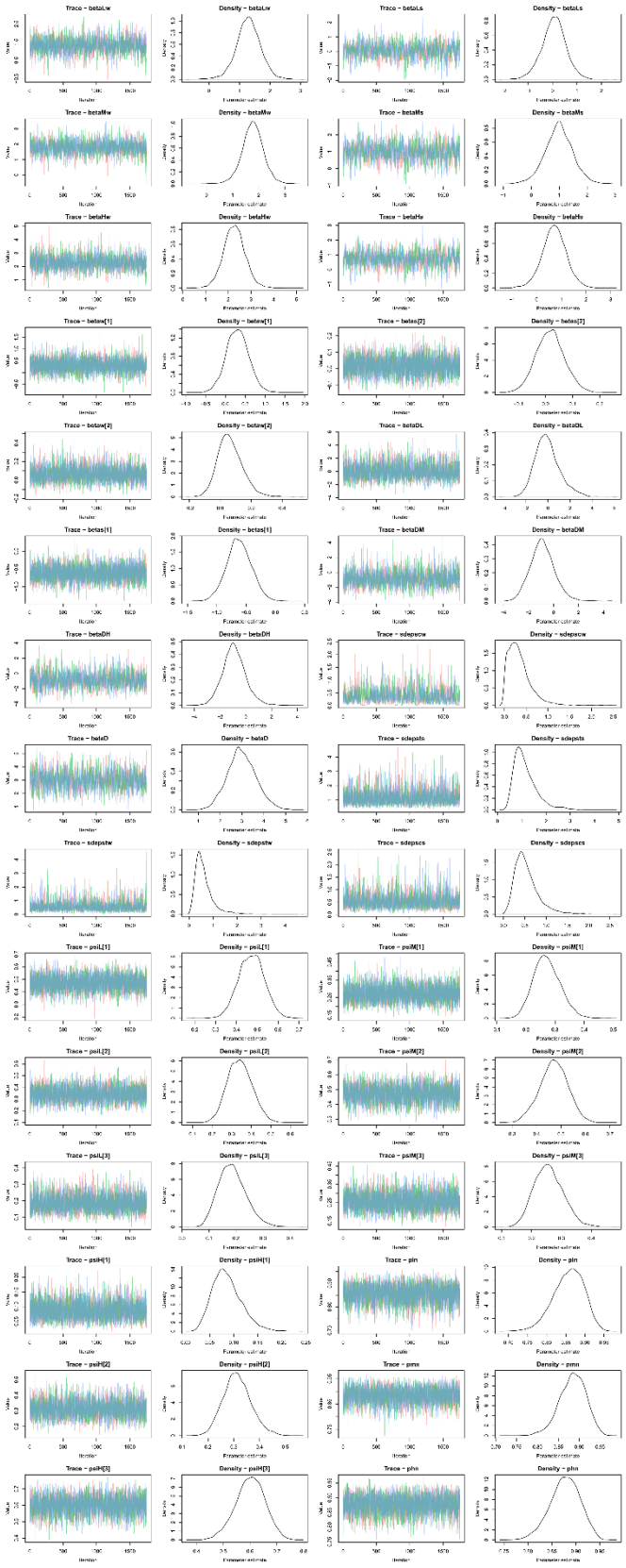

Figure S3. Trace plots and posterior density distributions for monitored parameters in the Bayesian multi-state capture–recapture model. Parameter notation corresponds to that described in Table S1

Model estimated values

Table S5. Multi-state capture-recapture model estimates. φ_{X_z} is the survival portability of an individual in state X (L low; M medium, H high) and time interval Z (W winter or S summer). β_{C_z} is the effect of the covariate C (Sex or Age) at time interval Z. $SD_{\varepsilon_{t_s}}$ is the standard deviation of random effect (ε_{r_z}) where r is the identity of the random effect (t year; Col colony) for the time period Z. p_{X_n} is the recapture probability at nets of an individual in state X. p_{X_f} is the recapture probability at RFID-feeders of an individual in state X. ψ_{XY} is the transition probability from state X to state Y from *t* to *t+1*. Columns represent mean, standard deviation (SD), lower (2.5%) and upper (97.5%) values of 95 confidence intervals, $\hat{R}$ and effective sample size (n.eff).

		mean	SD	2.50%	97.50%	$\hat{R}$	n.eff
Survival in winter	$Intercept_{\varphi_{L_w}}$	1.29	0.41	0.48	2.08	1.01	1,220
	$Intercept_{\varphi_{M_w}}$	1.77	0.41	0.93	2.56	1.01	1,302
	$Intercept_{\varphi_{H_w}}$	2.27	0.48	1.33	3.23	1.00	1,478
	β_{Sex_w}	0.30	0.28	-0.24	0.86	1.00	4,345
	β_{Age_w}	0.06	0.08	-0.07	0.24	1.00	3,435
	$SD_{\varepsilon_{t_w}}$	0.60	0.37	0.14	1.63	1.01	1,372
	$SD_{\varepsilon_{Col_w}}$	0.34	0.27	0.02	1.02	1.01	681
Survival in summer	$Intercept_{\varphi_{L_s}}$	0.05	0.50	-0.97	1.04	1.01	590
	$Intercept_{\varphi_{M_s}}$	0.99	0.50	-0.02	1.97	1.01	581
	$Intercept_{\varphi_{H_s}}$	0.71	0.50	-0.30	1.70	1.01	610
	β_{Sex_s}	-0.62	0.21	-1.04	-0.20	1.00	4,917
	β_{Age_s}	0.02	0.05	-0.08	0.12	1.00	5,250
	$SD_{\varepsilon_{t_s}}$	1.15	0.49	0.51	2.44	1.00	2,296
	$SD_{\varepsilon_{Col_s}}$	0.54	0.29	0.15	1.26	1.00	1,723
Detections at RFIDs	$Intercept_{p_{L_f}}$	-0.04	1.12	-1.95	2.54	1.00	2,610
	$Intercept_{p_{M_f}}$	-0.89	0.98	-2.67	1.16	1.00	1,449
	$Intercept_{p_{H_f}}$	-0.90	0.91	-2.60	1.04	1.00	1,457
	β_{RFID_f}	3.00	0.65	1.78	4.34	1.00	1,056
Detect. at nets	p_{L_n}	0.86	0.04	0.77	0.93	1.00	3,778
	p_{M_n}	0.88	0.03	0.82	0.94	1.00	3,797
	p_{H_n}	0.88	0.03	0.81	0.93	1.00	3,867
Status Transitions	ψ_{LL}	0.47	0.06	0.35	0.59	1.00	4,891
	ψ_{LM}	0.34	0.06	0.23	0.47	1.00	4,088
	ψ_{LH}	0.19	0.05	0.10	0.30	1.00	4,285
	ψ_{ML}	0.27	0.05	0.19	0.37	1.00	4,907
	ψ_{MM}	0.47	0.06	0.35	0.58	1.00	3,440
	ψ_{MH}	0.26	0.05	0.17	0.36	1.00	4,547

	ψ_{HL}	0.09	0.03	0.04	0.15	1.00	4,869
	ψ_{HM}	0.31	0.05	0.22	0.43	1.00	3,932
	ψ_{HH}	0.60	0.05	0.49	0.70	1.00	3,743

Posterior mean differences

Table S6. Posterior mean differences. Mean differences between the survival, transition, and recapture probabilities of the different social states (and their 95% confidence intervals) calculated from the posterior estimates. See Table S5 for parameter definitions.

	2.5%	**50%**	**97.5%**	**Significance**
$\boldsymbol{p_{H_f} - p_{M_f}}$	-0.538	-0.001	0.526	NO
$\boldsymbol{p_{H_f} - p_{L_f}}$	-0.687	-0.151	0.295	NO
$\boldsymbol{p_{M_f} - p_{L_f}}$	-0.720	-0.155	0.404	NO
$\boldsymbol{p_{H_n} - p_{M_n}}$	-0.088	0.030	0.158	NO
$\boldsymbol{p_{H_n} - p_{L_n}}$	-0.095	-0.006	0.077	NO
$\boldsymbol{p_{M_n} - p_{L_n}}$	-0.074	0.019	0.125	NO
$\boldsymbol{\varphi_{H_w} - \varphi_{M_w}}$	-0.034	0.049	0.149	NO
$\boldsymbol{\varphi_{H_w} - \varphi_{L_w}}$	0.015	0.118	0.251	YES
$\boldsymbol{\varphi_{M_w} - \varphi_{L_w}}$	-0.037	0.068	0.185	NO
$\boldsymbol{\varphi_{H_S} - \varphi_{M_S}}$	-0.172	-0.054	0.054	NO
$\boldsymbol{\varphi_{H_S} - \varphi_{L_S}}$	0.021	0.150	0.279	YES
$\boldsymbol{\varphi_{M_S} - \varphi_{L_S}}$	0.079	0.204	0.336	YES
$\boldsymbol{\psi_{LL} - \psi_{LM}}$	-0.095	0.134	0.343	NO
$\boldsymbol{\psi_{LL} - \psi_{LH}}$	0.097	0.288	0.462	YES
$\boldsymbol{\psi_{LM} - \psi_{LH}}$	-0.038	0.158	0.342	NO
$\boldsymbol{\psi_{ML} - \psi_{MM}}$	-0.371	-0.202	-0.014	YES
$\boldsymbol{\psi_{ML} - \psi_{MH}}$	-0.129	0.014	0.158	NO
$\boldsymbol{\psi_{MM} - \psi_{MH}}$	0.022	0.216	0.388	YES
$\boldsymbol{\psi_{HL} - \psi_{HM}}$	-0.363	-0.228	-0.094	YES
$\boldsymbol{\psi_{HL} - \psi_{HH}}$	-0.643	-0.517	-0.370	YES
$\boldsymbol{\psi_{HM} - \psi_{HH}}$	-0.479	-0.291	-0.066	YES

Repeatability

Table S7. Results of the Bayesian cumulative mixed model assessing repeatability in sociality level. Estimates are presented on the latent (logit) scale. Random-effect standard deviations were SD(id) = 1.27 [0.85, 1.71] and SD(colony) = 0.15 [0.00, 0.52].

	mean	SE	2.50%	97.50%	$\hat{R}$
$Intercept_{L-M_{treshold}}$	-0.66	0.14	-0.94	-0.38	1.00
$Intercept_{M-H_{treshold}}$	1.30	0.17	0.97	1.64	1.00
β_{Age}	0.11	0.04	0.02	0.20	1.00
β_{Sex}	-1.54	0.23	-2.02	-1.11	1.00

Sensitivity analysis

Sensitivity analysis - Model estimated values

Table S8. Multi-state capture–recapture model estimates from the sensitivity analysis using a 70% threshold to define strong social bonds. See Table S5 for parameter definitions.

		mean	SD	2.50%	97.50%	$\hat{R}$	n.eff
Survival in winter	$Intercept_{\varphi_{L_w}}$	1.16	0.46	0.07	1.97	1.01	681
	$Intercept_{\varphi_{M_w}}$	1.93	0.49	0.85	2.86	1.01	936
	$Intercept_{\varphi_{H_w}}$	2.16	0.51	1.10	3.16	1.01	951
	β_{Sex_w}	0.33	0.28	-0.22	0.90	1.00	4,533
	β_{Age_w}	0.07	0.08	-0.07	0.26	1.00	3,435
	$SD_{\varepsilon_{t_w}}$	0.64	0.44	0.13	1.76	1.01	720
	$SD_{\varepsilon_{Col_w}}$	0.36	0.27	0.02	1.01	1.01	1,014
Survival in summer	$Intercept_{\varphi_{L_s}}$	0.09	0.54	-1.03	1.17	1.00	429
	$Intercept_{\varphi_{M_s}}$	0.90	0.54	-0.19	1.98	1.00	455
	$Intercept_{\varphi_{H_s}}$	0.73	0.54	-0.39	1.81	1.00	416
	β_{Sex_s}	-0.63	0.22	-1.05	-0.21	1.00	5,250
	β_{Age_s}	0.01	0.05	-0.09	0.12	1.00	4,340
	$SD_{\varepsilon_{t_s}}$	1.15	0.48	0.53	2.40	1.00	1,809
	$SD_{\varepsilon_{Col_s}}$	0.51	0.29	0.11	1.25	1.00	1,607
Detections at RFIDs	$Intercept_{p_{L_f}}$	-0.11	1.12	-2.08	2.36	1.00	2,084
	$Intercept_{p_{M_f}}$	-1.04	0.99	-2.81	1.10	1.00	1,283
	$Intercept_{p_{H_f}}$	-0.76	0.98	-2.46	1.45	1.00	1,566
	β_{RFID_f}	3.02	0.66	1.72	4.31	1.00	929

Detect. at nets	p_{L_n}	0.87	0.04	0.78	0.93	1.00	3,594
	p_{M_n}	0.87	0.03	0.80	0.92	1.00	3,909
	p_{H_n}	0.89	0.03	0.82	0.94	1.00	3,739
Status Transitions	ψ_{LL}	0.50	0.06	0.38	0.62	1.00	4,308
	ψ_{LM}	0.32	0.06	0.21	0.45	1.00	3,652
	ψ_{LH}	0.17	0.05	0.09	0.27	1.00	3,921
	ψ_{ML}	0.30	0.05	0.22	0.40	1.00	4,852
	ψ_{MM}	0.44	0.06	0.33	0.55	1.00	3,776
	ψ_{MH}	0.25	0.05	0.17	0.35	1.00	4,424
	ψ_{HL}	0.11	0.03	0.06	0.18	1.00	4,960
	ψ_{HM}	0.30	0.05	0.21	0.42	1.00	3,577
	ψ_{HH}	0.58	0.05	0.47	0.68	1.00	3,928

Table S9. Multi-state capture–recapture model estimates from the sensitivity analysis using a 90% threshold to define strong social bonds. See Table S5 for parameter definitions.

		mean	SD	2.50%	97.50%	$\hat{R}$	n.eff
Survival in winter	$Intercept_{\varphi_{L_w}}$	1.15	0.45	0.20	1.98	1.03	771
	$Intercept_{\varphi_{M_w}}$	1.92	0.47	0.95	2.79	1.03	962
	$Intercept_{\varphi_{H_w}}$	2.17	0.52	1.14	3.19	1.02	924
	β_{Sex_w}	0.34	0.29	-0.20	0.91	1.00	4,163
	β_{Age_w}	0.08	0.09	-0.06	0.28	1.00	3,312
	$SD_{\varepsilon_{t_w}}$	0.61	0.43	0.11	1.67	1.07	809
	$SD_{\varepsilon_{Col_w}}$	0.37	0.32	0.01	1.18	1.06	540
Survival in summer	$Intercept_{\varphi_{L_s}}$	0.10	0.52	-0.96	1.08	1.01	487
	$Intercept_{\varphi_{M_s}}$	0.91	0.52	-0.12	1.91	1.01	512
	$Intercept_{\varphi_{H_s}}$	0.80	0.52	-0.25	1.79	1.00	503
	β_{Sex_s}	-0.61	0.22	-1.02	-0.17	1.00	4,884
	β_{Age_s}	0.01	0.05	-0.09	0.12	1.00	4,674
	$SD_{\varepsilon_{t_s}}$	1.13	0.50	0.52	2.35	1.02	2,136
	$SD_{\varepsilon_{Col_s}}$	0.53	0.31	0.11	1.33	1.00	1,557
Detections at RFIDs	$Intercept_{p_{L_f}}$	-0.21	1.09	-2.03	2.25	1.00	2,274
	$Intercept_{p_{M_f}}$	-0.71	1.03	-2.54	1.59	1.00	1,462
	$Intercept_{p_{H_f}}$	-1.00	0.91	-2.59	1.04	1.00	1,287
	β_{RFID_f}	3.03	0.63	1.82	4.28	1.00	993
Detect. at nets	p_{L_n}	0.86	0.04	0.77	0.93	1.00	3,410
	p_{M_n}	0.89	0.03	0.82	0.94	1.00	3,973
	p_{H_n}	0.87	0.03	0.80	0.93	1.00	3,413
Status Transitions	ψ_{LL}	0.47	0.06	0.34	0.60	1.00	4,297
	ψ_{LM}	0.37	0.07	0.25	0.50	1.00	3,319
	ψ_{LH}	0.16	0.05	0.08	0.27	1.00	4,299
	ψ_{ML}	0.27	0.05	0.19	0.37	1.00	4,928
	ψ_{MM}	0.42	0.05	0.32	0.53	1.00	3,916
	ψ_{MH}	0.30	0.05	0.21	0.41	1.00	4,682
	ψ_{HL}	0.10	0.03	0.05	0.17	1.00	4,353
	ψ_{HM}	0.31	0.06	0.21	0.43	1.00	3,117
	ψ_{HH}	0.59	0.05	0.48	0.69	1.00	3,480

Sensitivity analysis - Posterior mean differences

Table S10. Posterior mean differences from the sensitivity analysis using a 70% threshold to define strong social bonds. See Table S5 for parameter definitions.

	2.5%	50%	97.5%	Significance
$p_{H_f} - p_{M_f}$	-0.527	0.048	0.618	NO
$p_{H_f} - p_{L_f}$	-0.641	-0.122	0.390	NO
$p_{M_f} - p_{L_f}$	-0.722	-0.181	0.408	NO
$p_{H_n} - p_{M_n}$	-0.065	0.023	0.113	NO
$p_{H_n} - p_{L_n}$	-0.070	0.023	0.119	NO
$p_{M_n} - p_{L_n}$	-0.096	-0.001	0.100	NO
$\varphi_{H_w} - \varphi_{M_w}$	-0.065	0.021	0.121	NO
$\varphi_{H_w} - \varphi_{L_w}$	0.027	0.127	0.281	YES
$\varphi_{M_w} - \varphi_{L_w}$	0.002	0.106	0.249	YES
$\varphi_{H_S} - \varphi_{M_S}$	-0.157	-0.036	0.077	NO
$\varphi_{H_S} - \varphi_{L_S}$	0.018	0.142	0.277	YES
$\varphi_{M_S} - \varphi_{L_S}$	0.056	0.179	0.310	YES
$\psi_{LL} - \psi_{LM}$	-0.056	0.185	0.391	NO
$\psi_{LL} - \psi_{LH}$	0.146	0.334	0.502	YES
$\psi_{LM} - \psi_{LH}$	-0.037	0.150	0.331	NO
$\psi_{ML} - \psi_{MM}$	-0.320	-0.142	0.053	NO
$\psi_{ML} - \psi_{MH}$	-0.098	0.054	0.197	NO
$\psi_{MM} - \psi_{MH}$	-0.003	0.192	0.365	NO
$\psi_{HL} - \psi_{HM}$	-0.337	-0.194	-0.059	YES
$\psi_{HL} - \psi_{HH}$	-0.607	-0.475	-0.326	YES
$\psi_{HM} - \psi_{HH}$	-0.466	-0.285	-0.060	YES

Table S11. Posterior mean differences from the sensitivity analysis using a 90% threshold to define strong social bonds. See Table S5 for parameter definitions.

	2.5%	50%	97.5%	Significance
$p_{H_f} - p_{M_f}$	-0.613	-0.051	0.518	NO
$p_{H_f} - p_{L_f}$	-0.665	-0.137	0.314	NO
$p_{M_f} - p_{L_f}$	-0.677	-0.102	0.521	NO
$p_{H_n} - p_{M_n}$	-0.104	-0.017	0.072	NO
$p_{H_n} - p_{L_n}$	-0.082	0.011	0.118	NO
$p_{M_n} - p_{L_n}$	-0.065	0.028	0.133	NO
$\varphi_{H_w} - \varphi_{M_w}$	-0.067	0.023	0.125	NO
$\varphi_{H_w} - \varphi_{L_w}$	0.025	0.130	0.273	YES
$\varphi_{M_w} - \varphi_{L_w}$	0.002	0.109	0.241	YES
$\varphi_{H_S} - \varphi_{M_S}$	-0.144	-0.022	0.091	NO
$\varphi_{H_S} - \varphi_{L_S}$	0.027	0.154	0.287	YES
$\varphi_{M_S} - \varphi_{L_S}$	0.057	0.177	0.305	YES
$\psi_{LL} - \psi_{LM}$	-0.139	0.103	0.330	NO
$\psi_{LL} - \psi_{LH}$	0.117	0.309	0.482	YES
$\psi_{LM} - \psi_{LH}$	0.010	0.206	0.391	YES
$\psi_{ML} - \psi_{MM}$	-0.320	-0.151	0.022	NO
$\psi_{ML} - \psi_{MH}$	-0.184	-0.032	0.115	NO
$\psi_{MM} - \psi_{MH}$	-0.069	0.121	0.293	NO
$\psi_{HL} - \psi_{HM}$	-0.352	-0.204	-0.062	YES
$\psi_{HL} - \psi_{HH}$	-0.616	-0.494	-0.343	YES
$\psi_{HM} - \psi_{HH}$	-0.475	-0.290	-0.066	YES

Table S12. Posterior mean parameter estimates from the sensitivity analysis across strong-bond thresholds. See Table S5 for parameter definitions.

		Estimated value		
		70% threshold	**80% threshold**	**90% threshold**
Survival in winter	φ_{L_w}	0.75	0.78	0.74
	φ_{M_w}	0.87	0.85	0.86
	φ_{H_w}	0.89	0.90	0.89
Survival in summer	φ_{L_s}	0.52	0.51	0.52
	φ_{M_s}	0.70	0.72	0.69
	φ_{H_s}	0.66	0.66	0.67
Status Transitions	ψ_{LL}	0.50	0.47	0.47
	ψ_{LM}	0.32	0.34	0.37
	ψ_{LH}	0.17	0.19	0.16
	ψ_{ML}	0.30	0.27	0.27
	ψ_{MM}	0.44	0.47	0.42
	ψ_{MH}	0.25	0.26	0.30
	ψ_{HL}	0.11	0.09	0.10
	ψ_{HM}	0.30	0.31	0.31
	ψ_{HH}	0.58	0.60	0.59
Detect. at nets	p_{L_n}	0.87	0.86	0.86
	p_{M_n}	0.87	0.88	0.89
	p_{H_n}	0.89	0.88	0.87
Detect. at feeders	ψ_{LL}	0.49	0.48	0.46
	ψ_{LM}	0.28	0.32	0.36
	ψ_{HH}	0.35	0.31	0.30

Table S13. Statistical significance of posterior mean differences from the sensitivity analysis across strong-bond thresholds. Cells highlighted in red indicate cases in which the significance outcome differs from that obtained under the original model (80% strong-bond threshold). See Table S5 for parameter definitions.

	Significance 70%	Significance 80%	Significance 90%
$p_{H_f} - p_{M_f}$	NO	NO	NO
$p_{H_f} - p_{L_f}$	NO	NO	NO
$p_{M_f} - p_{L_f}$	NO	NO	NO
$p_{H_n} - p_{M_n}$	NO	NO	NO
$p_{H_n} - p_{L_n}$	NO	NO	NO
$p_{M_n} - p_{L_n}$	NO	NO	NO
$\varphi_{H_w} - \varphi_{M_w}$	NO	NO	NO
$\varphi_{H_w} - \varphi_{L_w}$	YES	YES	YES
$\varphi_{M_w} - \varphi_{L_w}$	YES	NO	YES
$\varphi_{H_S} - \varphi_{M_S}$	NO	NO	NO
$\varphi_{H_S} - \varphi_{L_S}$	YES	YES	YES
$\varphi_{M_S} - \varphi_{L_S}$	YES	YES	YES
$\psi_{LL} - \psi_{LM}$	NO	NO	NO
$\psi_{LL} - \psi_{LH}$	YES	YES	YES
$\psi_{LM} - \psi_{LH}$	NO	NO	YES
$\psi_{ML} - \psi_{MM}$	NO	YES	NO
$\psi_{ML} - \psi_{MH}$	NO	NO	NO
$\psi_{MM} - \psi_{MH}$	NO	YES	NO
$\psi_{HL} - \psi_{HM}$	YES	YES	YES
$\psi_{HL} - \psi_{HH}$	YES	YES	YES
$\psi_{HM} - \psi_{HH}$	YES	YES	YES

REFERENCES

Gelman, A., Carlin, J. B., Stern, H. S., Dunson, D. B., Vehtari, A., & Rubin, D. B. (2014). *Bayesian data analysis* (3rd ed.). CRC Press.

Griffiths, R., Double, M. C., Orr, K., & Dawson, R. J. G. (1998). A DNA test to sex most birds. *Molecular Ecology*, *7*(8), 1071–1075. https://doi.org/10.1046/j.1365-294x.1998.00389.x

Silva, N. J., Ferreira, A. C., Silva, L. R., Perret, S., Tieo, S., Renoult, J. P., Covas, R., & Doutrelant, C. (2025). Deep learning approach to detect and visualize sexual dimorphism in monomorphic species. *Animal Behaviour*, *225*, 123223. https://doi.org/10.1016/j.anbehav.2025.123223

van Dijk, R. E., Covas, R., Doutrelant, C., Spottiswoode, C. N., & Hatchwell, B. J. (2015). Fine-scale genetic structure reflects sex-specific dispersal strategies in a population of sociable weavers (Philetairus socius). *Molecular Ecology*, *24*(16), 4296–4311. https://doi.org/10.1111/mec.13308